Journal of Modern Technology and Engineering
Vol.7, No.2, 2022, pp.96-123

Jomard Publishing

STABILITY OF A CAR AS A HINGED-ROD SYSTEM UNDER THE ACTION OF COMPRESSIVE LONGITUDINAL FORCES IN A TRAIN

Angela Shvets*

Ukrainian State University of Science and Technologies, Dnipro, Ukraine

Abstract. The work is aimed to study the influence of longitudinal quasi-static compressive forces arising during stationary modes of train movement on the form of freight cars' instability. The relevance of this study relates to the need to control the longitudinal forces arising during the train movement, taking into account the increase in speeds, masses and lengths of trains, especially freight trains, by in the locomotives power increase. The use of the above methodology will improve the stability of freight rolling stock, justify the cause of derailment, as well as develop and put into practice technical measures to prevent the lift of the carriages, widening and shear of the track.

Keywords: traffic safety, car lift stability, longitudinal forces, transverse-longitudinal bending, compressed-bent rod, instability form.

Corresponding author: Angela Shvets, Department of Theoretical and structural mechanics, Ukrainian State University of Science and Technologies, Lazaryana St., 2, 49010, Dnipro, Ukraine, e-mail: *angela_shvets@ua.fm*

Received: 03 March 2022; Revised: 12 June 2022; Accepted: 29 June 2022; Published: 06 September 2022.

1 Introduction

Ensuring the car movement stability remains a pressing problem when increasing the movement speed and cancelling too rigid limitations on running long freight trains with increased carrying capacity (Kurhan et al., 2022; Kurhan & Kurhan, 2019; Kovalchuk et al., 2019).

Derailments of freight cars occur for various reasons: breakdown of equipment or individual parts; maintenance deviations in the track superstructure; incorrect order of passing and making-up trains; violation of normal dynamic conditions, which occurs due to hunting and unfavorable traffic conditions on a curved track section. In order to avoid derailments and ensure a stability coefficient, the restrictions expressed using certain indicators are set (Lysyuk, 2002; Sokol, 2002; Kampczyk & Dybel, 2021). These indicators determine the conditions for lifting the wheel above the rail head, overturning the rail and widening the railway track. One of the most widely used restrictions is the restriction expressed in terms of the ratio of the lateral force acting on the wheel to the vertical force L/V (Lazaryan et al., 1966; Vershinskiy, 1970; Shvets et al., 2016).

Numerous theoretical studies and expert practice demonstrate that it is the longitudinal compressive forces that, as a rule, contribute to the rolling stock derailment when the wheel flange is rolled onto the rail head. The presence of longitudinal forces in the train results in unloading the wheels moving along the outer rail line, and overloading the wheels moving along the inner rail line (Shvets et al., 2020, 2015; Wu et al., 2020).

Therefore, one of the priority tasks of improving the technology of driving trains is to study the influence of this force factor on the stability of freight cars in the working process (Kurhan et al., 2019; Shvets, 2021a; Zhang et al., 2021). Our aim s a theoretical study of the value of longitudinal forces of a quasi-static nature on the car instability form in a train.

2 Analysis of the latest research and the problem statement

When using a direct-acting locomotive brake, regenerative, rheostatic, emergency and full service brake applications, or when moving along a broken profile track, longitudinal compressive forces arise in the draw-and-buffer gears of the cars, which depend on the unit stiffness of the spring-friction gears, as well as the masses and movement speed of the interacting parts of the train (Lazaryan et al., 1966; Vershinskiy, 1970; Qi et al., 2012; Wu et al., 2016).

The unloading of any wheel caused by the action of dynamic longitudinal compressive forces, in combination with the unloading that occurs during the vibrations of the car body moving along the track, the content of which deviated from the established norms, can result in climbing the unloaded wheel flange onto the rail head with subsequent derailment (Fig. 1) (Lysyuk, 2002; Sokol, 2002; Lazaryan et al., 1966; Vershinskiy, 1970; Shvets et al., 2016, 2020, 2015).

Figure 1: Rolling stock derailment. a - derailment of freight cars in the Odessa region on the section Ivanivka - Veselyi Kut 03.07.2018; b- freight train derailment in West Midlands 13.09.2018

When moving, the car, under the action of longitudinal forces in automatic couplers, can take a different position relative to the track axle, which will largely determine both the values of the lateral horizontal forces of the wheel-rail interaction, the friction forces and wear of wheels and rails. Therefore, the longitudinal quasi-static (acting for more than 2 seconds) compressive force in the train is the main operational parameter (Sokol, 2002; Vershinskiy, 1970; Shaposhnik & Shikunov, 2021).

An important feature of a large number of operated models of undercarriage, which leads to an increased lateral influence of the wheel flanges on the rail head during the train braking, is the structural possibility of the transverse horizontal movement of the pivot section of the body relative to the track axle. Due to the gaps between the flanges and the rail head, as well as in the spring units, axle boxes and center plate arrangements, vehicle hunting, the eccentricities of the horizontal 5 and vertical Δ_i^y (Fig. 2) location of the coupler sockets relative to the nominal (design) longitudinal line, the bodies and automatic couplers of the carriages are located in the process of movement with some initial skews (Lysyuk, 2002; Sokol, 2002; Shvets, 2020).

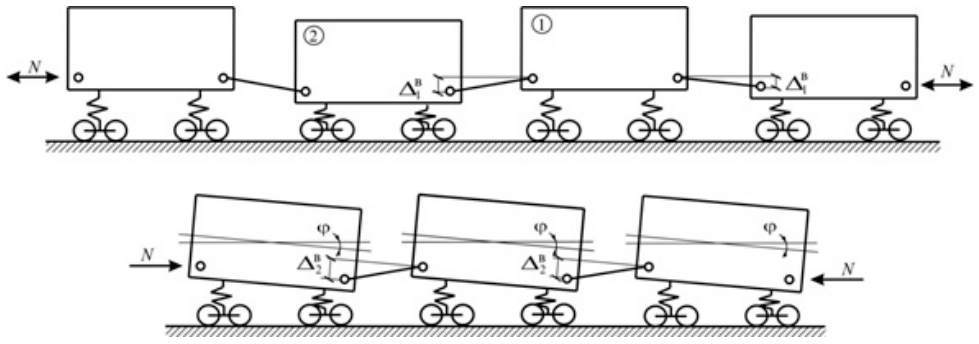

Figure 2: Layout of cars in a train during the car stability loss in a vertical plane

It is accepted that the stability loss characterized by the sudden appearance of qualitatively

new deformations, is called the first kind stability loss (Eulerian instability). Using the methods for calculating equilibrium systems, one can find the form of instability and the critical load.

The works Lysyuk (2002); Vershinskiy (1970); Vershinskiy et al. (1991) indicate that when studying a train as an articulated system, three forms of instability are possible. Fig. 3 demonstrates the interaction forces and the position of the central axle according to the three instability forms of the studied car under the action of compressive longitudinal forces.

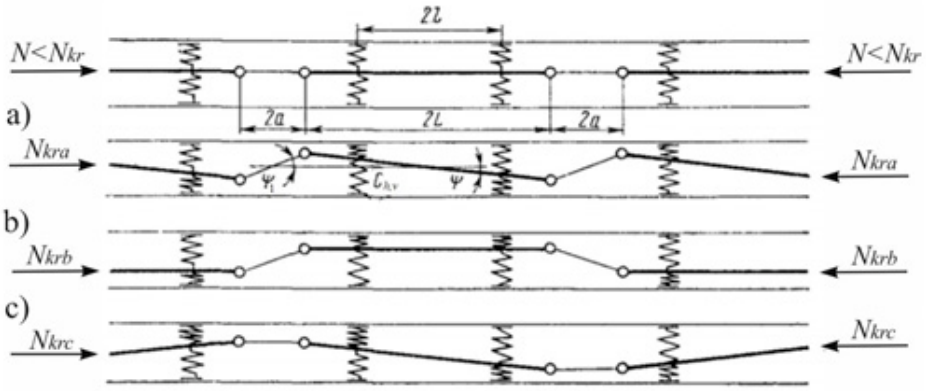

Figure 3: Layout of cars in the train in case of instability during the transfer of longitudinal force in the horizontal plane

Despite the fact that it has been established by theoretical studies that when the values of compressive forces are less than the critical one, the cars should not be lifted as a result of the train instability as a hinge-rod system. Practice shows that derailments occur in trains even with lower values of longitudinal forces. This is especially evident in trains with empty cars, which are characterized by intense wobbling in the operating speed range. Therefore, in addition to the longitudinal stability of the train as a hinge-rod system, for speeds exceeding the critical wobbling speed, in the presence of longitudinal compressive forces, one should consider the longitudinal-transverse stability of the movement of the system of cars in the train (Lysyuk, 2002; Vershinskiy, 1970; Vershinskiy et al., 1991).

Analyzing the derailments of freight trains in Fig. 1, one can assume that the derailment of 14 freight cars in the Odessa region on the Ivanivka – Veselyi Kut section on July 03, 2018 (Travel disruption as freight train derails near Coleshill, 2021) occurred during the instability of the II form (Fig. 1a). The derailment of a freight train in the West Midlands on September 13, 2018, is according to the I instability form (In the Odessa region, a freight train derailed, 2021) (Fig. 1b). In this regard, it is necessary to consider the existing analytical methods for determining the critical load under Eulerian instability and compare them with the longitudinal compressive forces arising in the train. To do this, one needs to know, among other things, the value of bending stiffness (elasticity) of the body and the automatic coupler.

In Vershinskiy et al. (1991), it is recommended to calculate the value of the critical force from the equilibrium condition of the system (cars in a train on a straight track section) in a state of skew under the action of longitudinal forces and reactions of transverse elastic couplings. The equilibrium equation for a skewed car, as shown in Fig. 3a:

$$\sum M = N_{kra} 2L\psi + N_{kra}\frac{2L^2}{a}\psi - 2\ell^2 C_{h,v}\psi = 0, \tag{1}$$

where ψ – is the rotation angle of the longitudinal axle of the car in the plan. In the same studies, the rotation angles of the car ψ and automatic coupler $\psi_i$were determined:

$$\psi = \frac{\delta_0}{\ell}, \tag{2}$$

$$\psi_1 = \psi_2 = \frac{\delta_0}{\ell}\left(1 + \frac{L}{a}\right). \tag{3}$$

Consider the definition of angles ψ, ψ_1 and ψ_2 in the horizontal plane during the compression of the car in the case of installation in a rut with the deviation of the body center plate across the path (in different directions from the longitudinal axle of the car) by the value δ_0 (Fig. 4) (Lysyuk, 2002; Vershinskiy, 1970; Shvets et al., 2020; Vershinskiy et al., 1991).

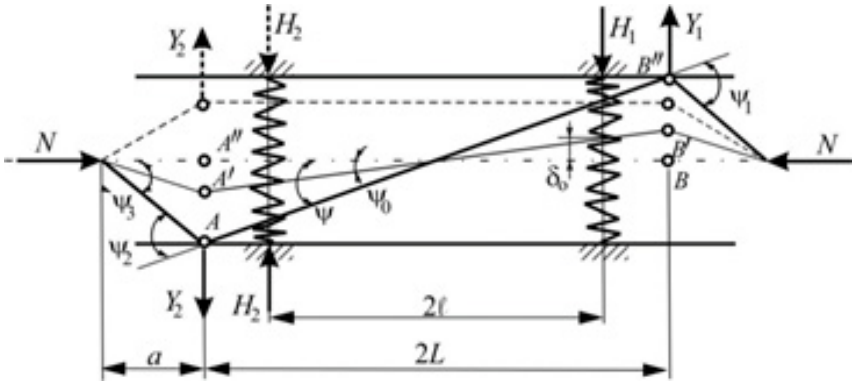

Figure 4: The scheme of the car to determine the components of the longitudinal forces in the horizontal plane

In Fig. 4, the dashed line shows the interaction forces and the position of the central axle with the chordal arrangement of the car under study under the action of compressive forces.

When the car axle is skewed (Fig. 3a) due to a lateral deflection from the track axle of the center plate section of the car frame due to the wheel set acceleration in the rail track, bearings are skewed along the axle necks, axle boxes – relative to the bogie frame ($BB' = A'A'' = \delta_0$), the car axle will additionally deflect due to spring deformation under the action of transverse components of longitudinal force ($B'B'' = A'A$). Let us find the rotation angles of the car body in the horizontal plane by dependencies (2)-(3).

It remains unexplained why, when solving equation (1), in relation to $N_{\mathrm{kr}a}$ the substitution was performed and, accordingly, the expression for the critical force was obtained:

$$\psi_1 = \psi_2 = \psi\frac{L}{a}, \tag{4}$$

$$N_{\mathrm{kr}a} = \frac{C_{h,v}}{1 + \frac{L}{a}} \cdot \frac{\ell^2}{L}. \tag{5}$$

Taking into account expression (3), the value of the critical force $N_{\mathrm{kr}a}$ should have the following form:

$$N_{\mathrm{kr}a} = \frac{C_{h,v}}{2 + \frac{L}{a}} \cdot \frac{\ell^2}{L}. \tag{6}$$

The values of critical forces for the cases shown in Fig. 3b,c are determined by the following dependencies:

$$N_{\mathrm{krb}} = a \cdot C_{h,v}, \tag{7}$$

$$N_{\mathrm{krc}} = C_{h,v} \cdot \frac{\ell^2}{L}. \tag{8}$$

To calculate the value of the critical longitudinal force, 12-532 gondola car was chosen on 18-100 three-element bogies. These cars have a low critical speed in terms of traffic stability, as well as the smallest tare weight, which leads to low stability under the action of compressive longitudinal forces. The designation of the parameters required for the calculations is summarized in Table 1.

Table 1: Parameters used in determining the resistance coefficient of car lift by longitudinal forces

Designation	Parameter	Dimension
N	longitudinal quasistatic force in an automatic coupler under the action of compressive forces on the car	kN
G_0	car body weight	kN
H_{f}	frame force acting on the wheel set	kN
G_{bog}	bogie weight	kN
$!_{\mathrm{h,v}}$	horizontal (vertical) stiffness of spring suspension of one bogie	kN/m
φ_1, φ_2	angles in the vertical plane due to the difference in levels of the automatic coupler axles in the connection of two cars	rad
Δ_1, Δ_2	difference in levels of the automatic coupler axles in front and behind the car	m
$2b$	the distance between the middle of the wheel set axle necks	m
$2\delta_0$	total lateral acceleration of the car body frame relative to the track axle in the guiding section along the center pin	m
2ℓ	wheel base	m
$2L$	distance between coupler followers	m
a	automatic coupler body length from pulling face to the shank end	m
$2S$	distance between wheel rolling circles	m
h_a	automatic coupler axle height above the rail heads level	m
h_{hs}	height above the rail heads plane to the upper plane of the central spring group	m
r	radius of a medium-worn wheel	m
h_{c}c	the height of the car gravity center above the rail heads level	m
h_{car}	height above the rail heads plane to the gravity center of the side surface of the car body	m
μ	wheel-rail friction coefficient	
β	inclination angle formed by the conical surface of the wheel flange to the horizontal axle	

Even for lightweight short-base cars, the correction of the value of the critical longitudinal force according to expression (6) does not have a significant effect – 3.21 MN and 2.83 MN, respectively. The values of critical forces according to (7) will be 8 MN, and according to (8) – 23.62 MN. In addition, when analyzing the analytical solution of the train stability problem as a hinge-rod system proposed in the works Lysyuk (2002); Vershinskiy (1970); Vershinskiy et al. (1991), the following inconsistencies arise:

1. It is proposed to consider the connection of two coupled automatic couplers as a single link, but when deriving the value of the critical longitudinal force, only one length of the automatic coupler body is used.

2. The force corresponding to the instability moment of the hinge-rod system is called critical by analogy with the Euler problem. The calculation of the critical force for freight cars is performed without taking into account the bending stiffness (elasticity) of the body and the automatic coupler.

3. When deriving the value of the critical force, the different initial state of the train is not taken into account, associated with the size of the gaps in the inter-car connections (automatic couplers) at the moment of the start of movement.

In works Lazaryan (1952, 1953, 1956) proposed to take into account the energy dissipation during vibrations and consider the train as a one-dimensional system of solid bodies connected by elastic-viscous bonds (Fig. 5a).

Numerous special experiments with trains made it possible to find many characteristics of freight and passenger trains necessary for calculations (the speed of the disturbance wave during

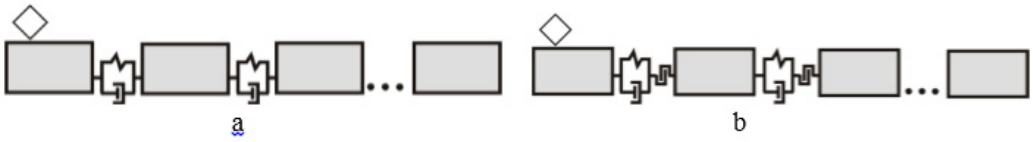

Figure 5: Design scheme of the train: a - in the form of a chain of bodies connected by elastic-viscous bonds; b - as a non-linear system.

starting-up and braking, the longitudinal stiffness of the train, the stiffness of automatic couplers during loading and unloading, as well as the average statistical values of the gaps in them).

The first studies of longitudinal forces, when gaps affect the transient process, were carried out experimentally. In work Lazaryan (1956) proposed as a design scheme a system of solid bodies, which are interconnected by elements with elastic imperfections, which take into account the gaps (Fig. 5b).

Design schemes of trains (Fig. 4) are distinguished by the presence of another element, which conditionally designates the gap in the automatic coupler and the nonlinearity of the power characteristics of the shock absorbing devices themselves. The presence of the gaps in the automatic couplers and, in the general case, the nonlinearity of the power characteristics of the shock absorbing devices of the automatic coupler makes us consider the train as a chain of solid bodies connected by the links with nonlinear characteristics (Lazaryan, 1985; Ursulyak & Shvets, 2017). The power characteristic of the inter-car connection (auto coupler) determines the stiffness during loading and unloading, that is, during the compression and tension of the train. The instability of cars in a train as a hinge-rod system originates from another type of deformation, namely from longitudinal-transverse bending. The value of stiffness for this type of deformation has other values and dimensions.

In Ushkalov (1965), it is indicated that the nominal bending stiffness of a gondola car body is approximately equal to three times the stiffness of the center sill (in the corresponding directions). The center sill of a four-axle gondola car is a structure of two Z-profile beams, on top of which an I-beam is welded along the entire length, which creates increased bending resistance. The values of the inertia moments of the gondola car center sill are given in Table 2.

Table 2: Profile for the center sills of cars

Profile	Reference value				
	Cross-sectional area A_x (cm^2)	Moment of inertia I_z (cm^4)	Moment of inertia I_y (cm^4)	x_0 (cm)	y_0 (cm)
Z no.31	84.74	13177.8	3760.95	13.05	15.37
I no.19	26.06	1438.55	53.42	3.75	9.50
Total	199.85	44197	55700	-	-

The modulus of elasticity for steel used in railway engineering is taken equal to: $E = 2.1 \cdot 10^5$ MPa. Stiffness of the car body is, respectively:
- $EI_z^c = 3 \cdot EI_z = 278441$ kN $\cdot$ m^2 in the vertical direction;
- $EI_y^c = 3 \cdot EI_y = 350910$ kN $\cdot$ m^2 in the horizontal direction.

In the article Shaposhnik & Shikunov (2021), the most unfavorable sections of the automatic coupler from the strength viewpoint are established. In accordance with the mechanical properties of the material of the automatic coupler body, the lowest bending stiffness in the area of the loop eyes of the automatic coupler body will be respectively:
- $EI_z^a = 3614$ kN $\cdot$ m^2 in the vertical direction;
- $EI_y^a = 472.5$ kN $\cdot$ m^2 in the horizontal direction.

When operating long trains, special attention is paid to the assessment of the dynamic performance of vehicles, among which the most important is the indicator that characterizes the

traffic safety of the vehicle – the derailment stability coefficient. For this purpose, mathematical models of spatial oscillations of a car (or a group of cars) moving as part of a train are used (Shvets, 2021a, 2020). In this case, the carriage model is divided into separate bodies and connections between them.

The modern rolling stock is a mechanical system with many degrees of freedom. The number of the freedom degrees depends on the design of the body support on the bogies, the number of axles, the design of the axle boxes, and the method of transmitting the traction force. To perform the calculations, the real structure is replaced by a design scheme, which should, if possible, fully reflect the studied properties of the structure. The stiffness of the body, wheel sets, bogie frames in railway vehicles is incomparably higher than that of the connection of their elastic suspension elements. Therefore, when studying vibrations, cars can be considered as mechanical systems consisting of absolutely solid bodies connected by elastic and rigid bonds (Lazaryan, 1985; Ushkalov, 1965).

The validity of this statement was proved in Lazaryan (1985); Ushkalov (1965); Shvets (2021b), where the body of a four-axle gondola car was considered as a discrete multi-mass system with elastic connections between the masses (Fig. 6).

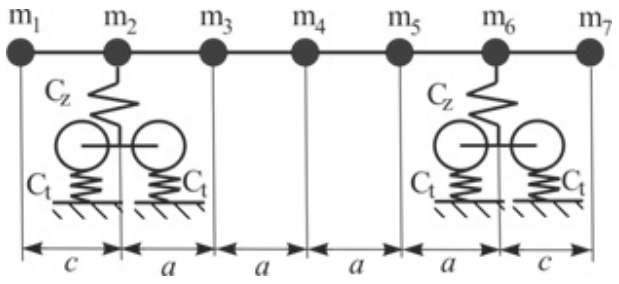

Figure 6: Design scheme of the body of a four-axle gondola car as an elastic massless beam

When studying the frequencies of natural bending vibrations, the body was considered as an elastic massless beam, and the mass of the body with the load was concentrated at seven points. The distribution of amplitudes for the three lowest bouncing oscillations showed that at the first frequency the body oscillates like a solid body. During the studies, the bending stiffness of the body varied within 0.75 and 100 stiffness of the gondola car center sill. It follows from the obtained solutions that the body elasticity practically does not affect the results of the solution of the problem on the car movement stability according to the first and second Lyapunov's theorems, and, therefore, the car body can be considered as an absolutely solid. The results of the study also made it possible to conclude that the elasticity of the rail base Ct and the bogie bolster does not significantly affect the natural frequencies of the bending vibrations of the bolster structure of a gondola car (Ushkalov, 1965; Shvets, 2021b).

As a result of extensive experimental studies of gondola car vibrations, it has been established that when moving along a track in good condition at a speed of up to 60 km/h, the spring sets of 18-100 three-element bogies and similar ones do not compress so that the sprung parts of four-axle gondola cars do not move relative to their unsprung parts. In the first approximation, it is considered that the vibrations are caused by the bending vibrations of the gondola car body as an elastic beam (Fig. 6), lying on two rigid (if the spring sets are not compressed and if the bolster is taken as a solid body) or on two elastic supports (when driving at speeds above 60 km/h).

The exact analytical solution of the problem of transverse-longitudinal bending of cars in a train, taking into account the real characteristics of spring-friction gears and automatic couplers, is very complex, time-consuming and requires special experiments (Sokol, 2002; Lazaryan, 1985; Ushkalov, 1965). In this regard, it is proposed to consider the existing analytical methods for determining the instability forms of a hinge-rod system that may occur in a train under the action of longitudinal compressive forces.

3 Experiment results

The work Blokhin & Vershinskiy (1985) presents an experimental assessment of the forces acting on the wheel sets of cars, depending on the value and sign of quasi-stationary longitudinal forces transmitted through the automatic couplers, when the cars move as part of a train along the straight and curved lines at low speeds (less than 50 km/h).

To carry out the experiments, an experimental train was formed, which consisted of a group of brake cars, an experimental coupling of cars, the brakes of which were turned off, diesel locomotives and laboratory cars. The group of the brake cars consisted of 6 loaded eight-axle tanks and 21 loaded four-axle gondola cars. The experimental coupling consisted of 7 gondola cars. In one cycle of experiments it was empty, in the other it was loaded. The gross weight of each car was 100 tons.

The main group of diesel locomotives, located near the experimental coupling, included one 4TE-10S four-section diesel locomotive and 2-3 (in different series of experiments) sections of 2TE-I0L diesel locomotive. An auxiliary group of diesel locomotives of 1-2 sections of 2TE-10L diesel locomotive was located behind the group of three laboratory cars. For safety reasons, 1-2 sections of 2TE-10L diesel locomotive were located at the head of the brake group. The brakes of the entire train were controlled from the cab of one of the diesel locomotives. The brakes of the experimental coupling and the laboratory cars were turned off and released. During the experiments, the train was braked by a given discharge stage (in different experiments from 0.04 to 0.18 MPa), the diesel locomotives immediately released themselves and then, on command, from 1 to 8 sections of the diesel locomotives developed traction forces, stretching or compressing the experimental coupling.

During the train movement, the speed changed in the range of 0-50 km/h. At the same time, as necessary, the discharge stage of the brake line during the movement increased. The longitudinal forces acting on the cars of the experimental coupling were of a quasi-stationary nature and were in the range of 0-2.7 MN. As a rule, smaller values of the forces corresponded to higher movement speeds, and vice versa, larger forces – to lower speeds. A number of experiments were carried out during the coasting period. The train was not braked, and the traction forces of the locomotives were turned off after speed up. The train was running on a section containing a straight line and two curves with radii of 400 and 700 m.

During the tests, the permissible level of the longitudinal forces, in some cases, was exceeded. In the empty mode, the car of the experimental coupling derailed at a compressive force of 1.4 MN due to mounting of the unloaded wheel onto the rail (Fig. 7).

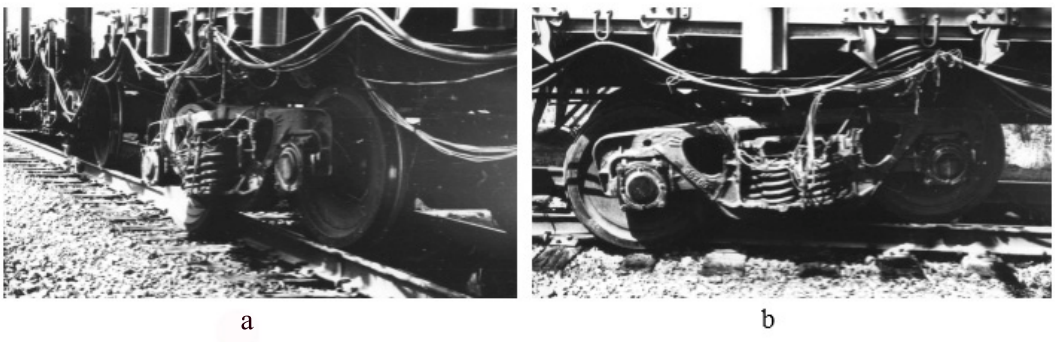

Figure 7: Derailment of the car of the experimental coupling: a- derailment of the front bogie of the car of the experimental coupling; b - side view of the derailed bogie

In the loaded mode, it was not possible to achieve a car derailment, since 4TE-10S diesel locomotive turned out to be the limiting one. With a compressive longitudinal force approximately equal to 2.5 MN, due to the action of the significant horizontal transverse forces the rail overturning under it took place (Fig. 8).

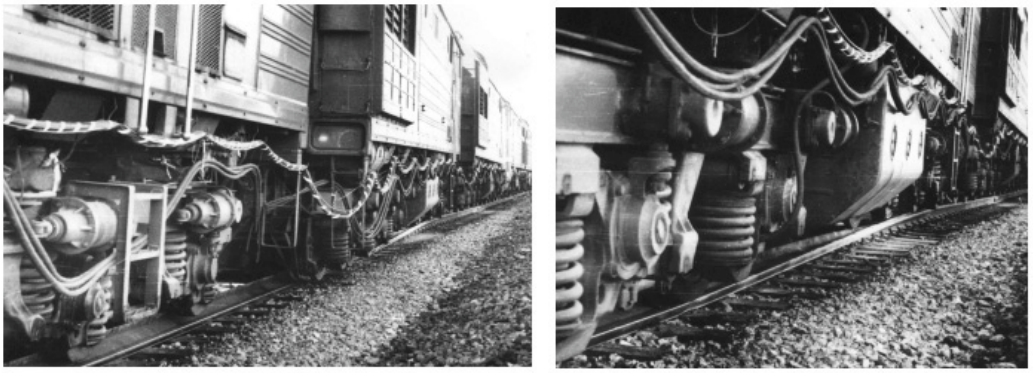

Figure 8: Derailment of 4TE-10S diesel locomotive: a- general view of the experimental train; b- rail overturning under the locomotive.

The patterns of both derailments, in general, corresponded to the research data Vershinskiy (1970); Vershinskiy et al. (1991), in particular, the carriages were in the position of the greatest skew in the track (according to II form, Fig. 9a), and their rotation angles in the plan (hunting angles) were of the same sign (herringbone pattern, Fig. 9b)

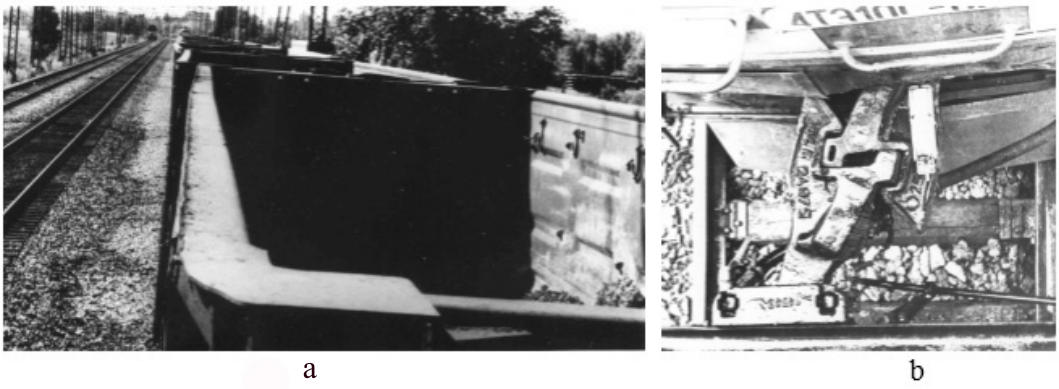

Figure 9: Experimental coupling of empty gondola cars: a- the position of the greatest skew of cars in the track; b- top view of the automatic coupling equipment of an experimental car coupling

During the experiments for the cars of the experimental coupling, the transverse (to the track axle) forces were measured – horizontal, acting on the wheel sets, and vertical in the supports of the bolsters, as well as longitudinal forces in automatic couplers. In Blokhin & Vershinskiy (1985), an increase in the transverse forces with an increase in the longitudinal force modulus is noted.

4 Stability of a freight car in a train under the action of the compressive longitudinal forces

A large number of studies have been devoted to traffic safety issues and criteria for determining the stability of rolling stock movement, which shows the relevance of this research area. The following methodology for determining the criterion of wheel derailment stability was published in the works Shvets et al. (2016, 2020); Shvets (2020). The previous conclusions of dependencies for determining the vertical and transverse rail response to the climbing wheel are given in relation to a straight track section.

The basis of the methodology for determining the lift resistance coefficient by the longitudinal

forces is the research presented in the works Shvets et al. (2016, 2020); Shvets (2020). The carriage movement in the curve is considered at different angles on both sides of the car: the tilt angles of the bodies to the track plane φ_1 and φ_2; automatic coupler rotation angles relative to the track axle ψ_1 and ψ_2; the car body rotation within the gap in the track by an angle ψ is taken into account. The car (Fig. 10) is subject to compressive longitudinal forces, and the carriage is placed on the rail track according to the maximum skew-symmetrical skew scheme. The longitudinal forces N_1 and N_2, acting in automatic couplings in front and behind the car, are assumed to be the same.

The forces acting on the car are projected on the track plane, as well as on the planes perpendicular to it – longitudinal and transverse relative to the track axle. The designations given in Fig. 10, as well as the parameters used to determine the resistance coefficient of car lift by longitudinal forces, are summarized in Table 1. The efforts depicted in Fig. 4 are determined according to the methodology given in the works Shvets et al. (2020); Shvets (2020).

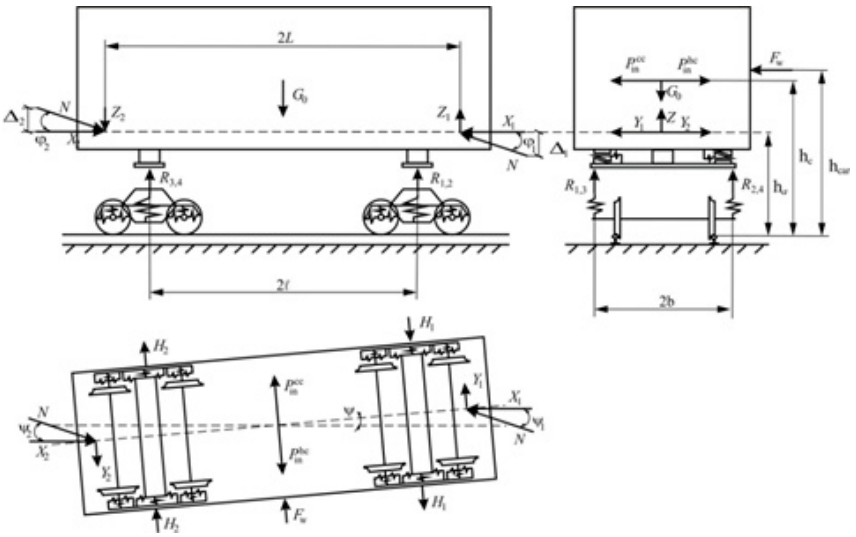

Figure 10: Scheme of forces acting on the car (II form of instability)

The angles in the vertical plane due to the difference in levels of the automatic coupler axles in the connection of two cars:

$$\varphi_1 = \frac{\Delta_1}{2a},\ \varphi_2 = \frac{\Delta_2}{2a}. \tag{9}$$

Since the angles ψ, ψ_1 and ψ_2 depend on the argument δ_0, which in turn depends on frame force acting on the wheel set H_{f}, the calculation by equations (2)-(3) is possible by the method of successive approximations. With sufficient accuracy for calculation, it is possible to limit ourselves to the first approximation and equations (2)-(3), taking into account the elastic transverse deformation of the spring sets of the bogies, will take the following form in a straight track section:

$$\psi = \frac{\delta_0}{\ell} \cdot \left[1 + \frac{N \cdot L}{2\ell^2 \cdot C_{\mathrm{h}}} \left(2 + \frac{L}{a}\right)\right], \tag{10}$$

$$\psi_1 = \psi_2 = \frac{\delta_0}{\ell} \cdot \left[1 + \frac{N \cdot L}{2\ell^2 \cdot C_{\mathrm{h}}} \left(2 + \frac{L}{a}\right)\right] \cdot \left(1 + \frac{L}{a}\right), \tag{11}$$

The vertical and horizontal forces acting on the wheel set are determined from the balance of the unsprung part of the bogie. As a result of solving a system of linear equations, we determine the vertical and lateral transverse reaction of the rail to the climbing wheel, as well as the lift

resistance coefficient by longitudinal forces.

$$V = \frac{G_0}{8} + \frac{G_{\text{bog}}}{4} + \frac{N}{8} \times \\ \times \left[(\psi_1 - \psi_2) \cdot \frac{h_a}{S} - \left[\varphi_1 \cdot \left(\frac{L}{\ell} + 1 \right) + \varphi_2 \cdot \left(\frac{L}{\ell} - 1 \right) \right] \cdot \frac{b}{S} + (\psi_1 + \psi_2 + 2\psi) \cdot \frac{L \cdot h_{\text{hs}}}{\ell \cdot S} \right], \tag{12}$$

$$L = \mu \cdot \left(\frac{G_0}{8} + \frac{G_{\text{bog}}}{4} \right) + \frac{N}{8} \times \\ \times \left[\begin{array}{l} (\psi_1 - \psi_2) \cdot \left(2 - \mu \cdot \frac{h_a}{S} \right) - \mu \cdot \left[\varphi_1 \cdot \left(\frac{L}{\ell} + 1 \right) + \varphi_2 \cdot \left(\frac{L}{\ell} - 1 \right) \right] \cdot \frac{b}{S} + \\ + (\psi_1 + \psi_2 + 2\psi) \cdot \frac{L}{\ell} \cdot \left(2 - \mu \cdot \frac{h_{\text{hs}}}{S} \right) \end{array} \right], \tag{13}$$

$$C_{\text{lr}} = \frac{tg\beta - \mu}{1 + \mu \cdot tg\beta} \cdot \frac{P_{\text{car}} + N \cdot \left[(\psi_1 - \psi_2) \cdot \frac{h_a}{S} - \varphi_{\text{e}} \cdot \frac{b}{S} + (\psi_1 + \psi_2 + 2\psi) \cdot \frac{L \cdot h_{\text{hs}}}{\ell \cdot S} \right]}{\mu \cdot P_{\text{car}} + N \cdot \left[(\psi_1 - \psi_2) \cdot \left(2 - \mu \cdot \frac{h_a}{S} \right) - \mu \cdot \varphi_{\text{e}} \cdot \frac{b}{S} + (\psi_1 + \psi_2 + 2\psi) \cdot \frac{L}{\ell} \cdot \left(2 - \mu \cdot \frac{h_{\text{hs}}}{S} \right) \right]}. \tag{14}$$

The dependency for determining the resistance coefficient of car lift by longitudinal forces in a straight track section has the following form:

$$C_{\text{lr}} = \frac{tg\beta - \mu}{1 + \mu \cdot tg\beta} \cdot \frac{P_{\text{car}}^{\text{st}} + \frac{N^2}{l_{\text{h}}} \cdot \frac{\psi_0^2 \cdot h_{\text{hs}}}{\delta_0 \cdot S} + N \cdot 2\psi_0 \cdot \frac{h_{\text{hs}}}{S}}{\mu \cdot P_{\text{car}}^{\text{st}} + \frac{N^2}{l_{\text{h}}} \cdot \frac{\psi_0^2}{\delta_0} \cdot \left(2 - \mu \cdot \frac{h_{\text{hs}}}{S} \right) + N \cdot 2\psi_0 \cdot \left(2 - \mu \cdot \frac{h_{\text{hs}}}{S} \right)}. \tag{15}$$

Where $P_{\text{car}}^{\text{st}}$ – is the static pressure of the car, taking into account unloading from longitudinal force, kN. $P_{\text{car}} = G_{\text{o}} + 2G_{\text{bog}}$ – car weight, kN; φ_{e} – the rotation angle of the car body in a vertical plane, caused by the presence of a difference in the levels of automatic coupler axles in front and behind the car, rad.

The most unfavorable schemes for applying compressive longitudinal forces in the vertical plane (Shvets, 2020) are shown in Fig. 11.

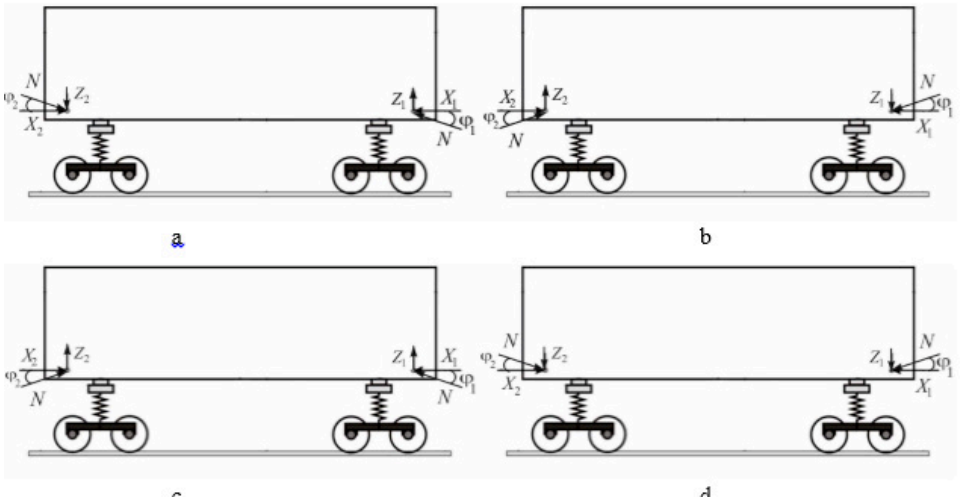

Figure 11: Schemes for applying projections of longitudinal forces in the vertical plane: a-b opposite directed; c-d unilaterally directed

For these cases, the dependence for determining the lift resistance coefficient by longitudinal forces (15) will have differences in the expressions for determining the equivalent rotation angle from the action of the vertical components of the longitudinal force and the static pressure of the car, taking into account the unloading from the longitudinal force $P_{\text{car}}^{\text{st}}$ for the front and rear bogies respectively.

Front bogie of the car:

$$P_{\text{car}}^{\text{st}} = P_{\text{car}} \mp N \cdot \varphi_{\text{e}} \cdot \frac{b}{S}, \tag{16}$$

$$\varphi_{\text{e}} = \varphi_1 \cdot \left(\frac{L}{\ell} + 1\right) \pm \varphi_2 \cdot \left(\frac{L}{\ell} - 1\right). \tag{17}$$

For the schemes of application of longitudinal forces presented in Fig. 11a,b, dependence (17) is used with a + sign, and for the schemes in Fig. 11c,d, with a – sign. The static pressure of the car, taking into account the unloading from the longitudinal force according to dependence (16), is determined for the application schemes of the longitudinal forces in Fig. 11a,c – with a – sign, and for Fig. 11b,d – with a + sign.

Front bogie of the car:

$$P_{\text{car}}^{\text{st}} = P_{\text{car}} \pm N \cdot \varphi_{\text{e}} \cdot \frac{b}{S}, \tag{18}$$

When determining the lift resistance coefficient by longitudinal forces on the inner rail line for the application schemes of longitudinal forces shown in Fig. 11a,b, dependence (17) is used with a + sign, and for the schemes in Fig. 11c,d, with a – sign. The static pressure of the car, taking into account the unloading from the longitudinal force $P_{\text{car}}^{\text{st}}$according to dependence (18), is determined for the application schemes of the longitudinal forces in Fig. 11a,c – with a + sign, and for Fig. 11b,d – with a – sign.

ψ_a – the angle formed by the longitudinal axle of the automatic coupler body and the axle of the central sill of the car frame in a horizontal plane, rad:

$$\psi_0 = \frac{\delta_0 \cdot L}{\ell^2} \cdot \left(2 + \frac{L}{a}\right), \tag{19}$$

$h_{\text{hs}} = r + r_{\text{n}} \approx r$ – height above the level of the rail heads plane to the upper plane of the central spring set, m. Often this parameter in a number of studies is taken equal to the radius of the average worn wheel.

Previously, it was noted that when testing in an empty mode, the derailment of the car of the experimental coupling was noted at a compressive force of 1.4 MN due to the unloaded wheel mounting onto the rail (Blokhin & Vershinskiy, 1985). At the same time, it has been repeatedly noted that the derailment of empty cars occurs with a longitudinal compressive force of 500-600 kN. At the time of the dynamic running tests, the permissible difference in the heights of the axles of two adjacent cars in the case of non-central interaction was allowed to be 0.1 m. For comparison, let us calculate the stability of the car wheel set under the action of compressive longitudinal forces according to dependence (15) using the relations (16)-(17) with a difference in the axles of two neighboring cars. The calculations took into account the difference in height between the longitudinal axles of automatic couplers in a freight train from 0 to 0.1 m with a step of 0.02 m. Behind the car under study, the difference between the axle levels of the automatic couplers is taken equal to Δ_2=0.04 m in Fig. 12a,b and Δ_2=0 in Fig. 12c,d.

The results given confirm that the wheel flange climbing onto the rail head with the subsequent fall of the other wheel inside the track in an empty car, described in (Shvets, 2021b), occurred during the train braking, when the car is lifted and at the same time is set according to the II instability form (herringbone) under the action of oncoming cars. The car bodies of the experimental coupling most likely initially lost their stability on the springs of the central spring suspension in the vertical plane. It is obvious that the derailed car body, after stability loss, loaded the front bogie in the movement direction. Consequently, the stability loss of freight cars as part of a train should be divided into two stages: stability loss of the body on suspension springs and the stability loss of the wheel set, which results directly in the derailment.

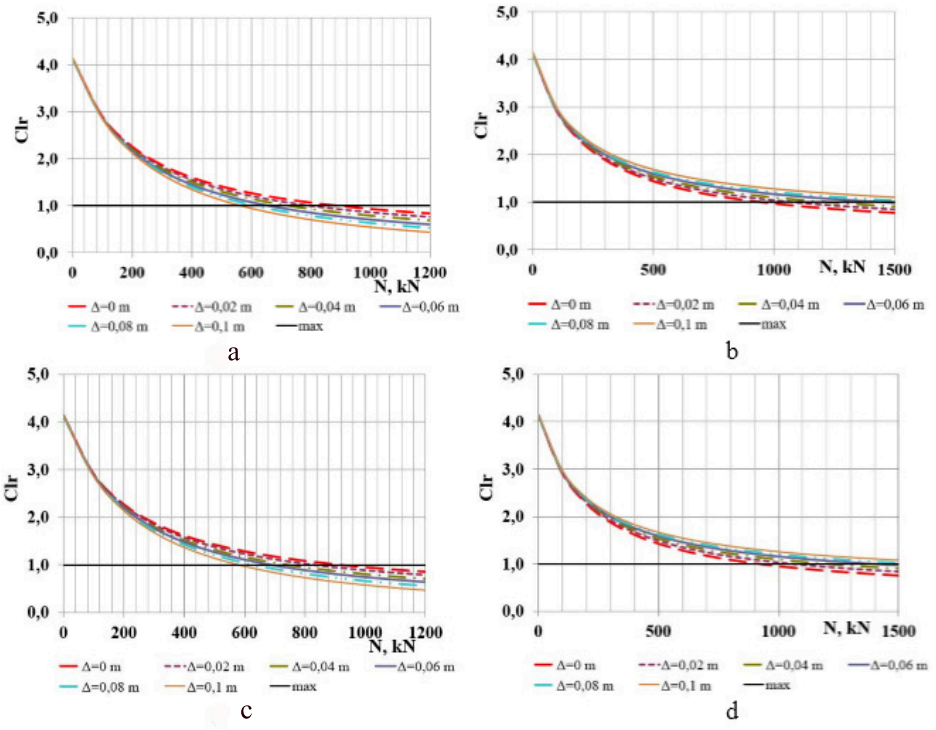

Figure 12: Resistance coefficient of an empty open car lift: a-c unloaded front bogie; b-d loaded front bogie

5 Results of analytical studies

Numerous studies have been devoted to the elastic stability theory; they cannot be listed within the framework of one study. In the given work, only some methods for determining the stability of articulated systems under the action of a compressive longitudinal load are considered (Klein et al., 1972; Shaukat et al., 2021; Zhang et al., 2022; Rabinovich, 1960; Volmir, 1967; Darkov & Shaposhnikov, 1986; Prokofiev & Smirnov, 1948).

When conducting analytical studies, it is assumed that:

1. Longitudinal forces in front and behind the car are assumed to be equal in value.

2. Since the stiffness of the body, wheel sets, bogie frames in railway vehicles is incomparably higher than that of the connection of their elastic suspension elements, the freight car is considered as a mechanical system consisting of absolutely rigid bodies connected by elastic links.

3. Since the bogie bolster elasticity does not have a noticeable effect on the natural frequencies of the bending vibrations of the bolster structure of the gondola car, the car is considered as a beam consisting of three absolutely rigid links hinged to each other supported by elasto-yielding supports with the same stiffness coefficient.

4. The different initial state of the train related to the value of the gaps in the automatic couplers at the time of the start of movement is not taken into account.

5.1 System stability with two degrees of freedom

The work Klein et al. (1972) considers a beam consisting of three absolutely rigid links hinged to each other. Supports A and B do not allow vertical movements, supports K and M are elasto-yielding with the same stiffness coefficient. The system is under the action of a compressive longitudinal force, which leads to the displacement of hinges C and D. Let us determine the load at which some deviated equilibrium state is possible. The support reactions of the new equilibrium state are shown in Fig. 13.

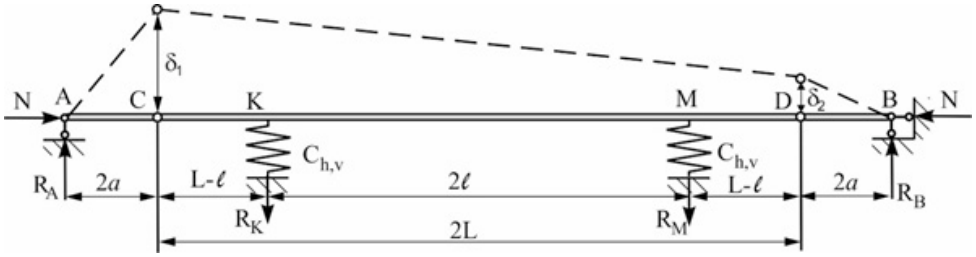

Figure 13: Schematic representation of a freight car of three absolutely rigid links hinged to each other

Static method. Since the system has two degrees of freedom, it suffices to compose two equilibrium equations. A system of two homogeneous equations can have a zero solution for the unknowns $\delta_1 = \delta_2 = 0$, which corresponds to a horizontal equilibrium state. We obtain a nonzero solution if we equate the determinant composed of the coefficients of the following unknowns to zero:

$$D = \begin{vmatrix} \left[\frac{C_{h,v}2a\cdot\left(2aL+L^2+\ell^2\right)}{L(4a+2L)} - N\right]\cdot\delta_1 & \left(2aL+L^2-\ell^2\right)\frac{C_{h,v}2a}{L(4a+2L)}\cdot\delta_2 \\ \left(2aL+L^2-\ell^2\right)\frac{C_{h,v}2a}{L(4a+2L)}\cdot\delta_1 & \left[\frac{C_{h,v}2a\cdot\left(2aL+L^2+\ell^2\right)}{L(4a+2L)} - N\right]\cdot\delta_2 \end{vmatrix} = 0. \tag{20}$$

Expanding the determinant, we obtain a quadratic equation for determining the critical force and its two values:

$$N_{\mathrm{kr1}} = N_{\mathrm{krb}} = 2a\cdot C_{h,v}, \tag{21}$$

$$N_{\mathrm{kr2}} = N_{\mathrm{kra}} = \frac{C_{h,v}\cdot 2a\cdot\ell^2}{L\cdot(2a+L)} = \frac{2C_{h,v}}{2+\frac{L}{a}}\cdot\frac{\ell^2}{L}. \tag{22}$$

Energy method. Considering the deformed equilibrium state, we equate to zero the sum of the work of external and internal forces $A + W = 0$ to zero and, having solved the equation for N_{kr}, we obtain:

$$N_{\mathrm{kr}} = \frac{C_{h,v}\cdot a}{L}\cdot\frac{\left(\delta_1^2+\delta_2^2\right)\left(L^2+\ell^2\right)+2\delta_1\delta_2\left(L^2-\ell^2\right)}{\left(\delta_1^2+\delta_2^2\right)(a+L)-2a\delta_1\delta_2}. \tag{23}$$

If $\delta_1 = \delta_2$, we obtain dependence (21), and if $\delta_1 = -\delta_2$, we obtain dependence (22).

Thus, the obtained solution proves:

- the value of the critical forces according to (5)-(8) was obtained for a beam on elasto-yielding supports;
- when taking into account two coupled couplers as a single link, the value of the critical force doubles and takes an irrationally large value;
- confirms the correctness of expression (6);
- when deriving the dependence to determine the critical force, the possible displacement of supports A and B is not taken into account, which leads to the need to consider the stability of a car group as part of a train;
- demonstrates the following inconsistency – in this way it is possible to obtain two instability forms, and not three as it was previously indicated.

5.2 Finite difference method (FDM)

Structurally, the connection of the automatic coupler with the car frame is neither a perfectly articulated nor a perfectly rigid node. Such nodes are considered as flexible, allowing mutual displacement of the elements that are being connected. Let us determine the approximate value of the critical force for a freight car as for a compressed rod of variable stiffness on elastic supports (Fig. 14).

The finite difference method is an approximate method that refers to the static stability criterion (Rabinovich, 1960; Volmir, 1967). The second derivative for the differential equation of the bent axle of the beam for some point separating two adjacent intervals can be replaced approximately using the central difference:

$$EI_i \frac{1}{\ell_i^2} \cdot (v_{i-1} - 2v_i + v_{i+1}) = -Nv_i. \tag{24}$$

where EI_i – the value of the rod stiffness on the considered interval; v_{i-1}, v_i, v_{i+1} – deflections at relevant points. Such equations can be compiled $(n-1)$, where n is the number of intervals in the articulated chain and they will include the deflections values at the end points. Thus, we obtain a system $(n-1)$ of algebraic equations in relation to v_i. The compatibility condition for these equations (for a nonzero solution) leads to the definition of the critical load.

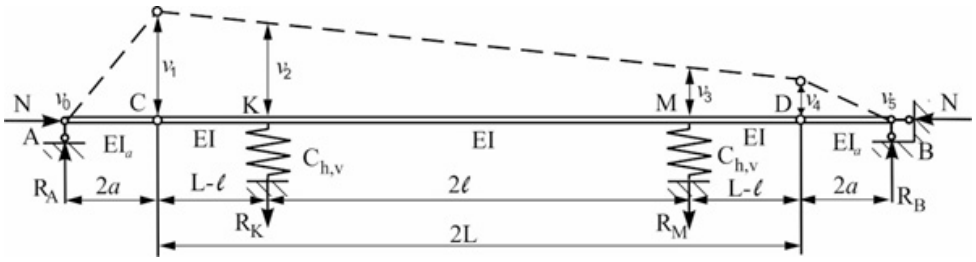

Figure 14: Scheme of a freight car during the calculation by the finite difference method

The system of algebraic equations in relation to v_i for 4 sections in Fig. 14 will have the form:

$$\left[\alpha \frac{4a^2}{k} - 2\right] \cdot v_1 + v_2 = 0, \tag{25}$$

$$v_1 + \left[\alpha (L-\ell)^2 - 2\right] \cdot v_2 + v_3 = 0, \tag{26}$$

$$v_2 + \left[\alpha 4\ell^2 - 2\right] \cdot v_3 + v_4 = 0, \tag{27}$$

$$v_3 + \left[\alpha (L-\ell)^2 - 2\right] \cdot v_4 = 0. \tag{28}$$

Equating the determinant of the system of equations (25)-(28) to zero, we obtain the characteristic equation in relation to α. Loss of stability in the horizontal direction at $k = 0.0013$:

$$D = \begin{bmatrix} 3076.923\alpha - 2 & 1 & 0 & 0 \\ 1 & 4.08\alpha - 2 & 1 & 0 \\ 0 & 1 & 74.996\alpha - 2 & 1 \\ 0 & 0 & 1 & 4.08\alpha - 2 \end{bmatrix} = 0. \tag{29}$$

$$303.096\alpha^4 - 303.983\alpha^3 + 78.21\alpha^2 - \alpha + 3.907 \cdot 10^{-4} = 0, \tag{30}$$

$$\alpha_{kr1} = 0.4878,\ \alpha_{kr2} = 0.0131,\ \alpha_{kr3} = 0.5017,\ \alpha_{kr4} = 0.0004. \tag{31}$$

The smallest value of the critical force according to the approximate finite difference method will be 140.4 kN.

Method of elastic articulated chain. This method is another variant of the finite difference method and consists in the fact that the differential equation, for a hinged rod, represented through the difference "taken in advance", has the form:

$$\frac{\Delta (v_{i+1} - v_i)}{\ell_i^2} = -\frac{N}{EI_i} v_i. \tag{32}$$

Displacements v_i (Fig. 14) are determined sequentially using expressions:

$$\Delta v_2 = \Delta v_1 - \frac{N4a^2}{kEI} v_1 = \Delta v_1 - \frac{\alpha 4a^2}{k} v_1, \tag{33}$$

$$\Delta v_3 = \Delta v_2 - \frac{N\left(L-\ell\right)^2}{EI}\left(v_1+v_2\right) = \Delta v_2 - \alpha\left(L-\ell\right)^2 \cdot \left(v_1+v_2\right), \tag{34}$$

$$\Delta v_4 = \Delta v_3 - \frac{N4\ell^2}{EI}\left(v_2+v_3\right) = \Delta v_3 - \alpha 4\ell^2 \cdot \left(v_2+v_3\right). \tag{35}$$

Considering $\Delta v_1 = v_1$, we obtain:

$$v_2 = v_1 + \Delta v_2 = 2v_1 - \frac{\alpha 4a^2}{k} v_1, \tag{36}$$

$$v_3 = v_2 + \Delta v_3 = 3v_1 - \frac{\alpha 8a^2}{k} v_1 - 3\alpha\left(L-\ell\right)^2 v_1 + \frac{\alpha^2\left(L-\ell\right)^2 4a^2}{k} v_1, \tag{37}$$

$$\begin{aligned} v_4 = v_3 + \Delta v_4 = 4v_4 - \tfrac{\alpha 12a^2}{k} v_1 - 6\alpha\left(L-\ell\right)^2 v_1 + \tfrac{8\alpha^2 a^2 (L-\ell)^2}{k} v_1 - 20\alpha\ell^2 v_1 + \\ + \tfrac{48\alpha^2 a^2 \ell^2}{k} v_1 + 12\alpha^2\ell^2\left(L-\ell\right)^2 v_1 - \tfrac{16\alpha^3\ell^2 a^2 (L-\ell)^2}{k} v_1. \end{aligned} \tag{38}$$

Loss of stability in the vertical direction at $v_4 = -v_1$ and $k = 0.013$:

$$\begin{aligned} &16\alpha^3\ell^2 a^2\left(L-\ell\right)^2 - \alpha^2\left[8a^2\left(L-\ell\right)^2 + 48a^2\ell^2 + 12k\ell^2\left(L-\ell\right)^2\right] + \\ &+\alpha\left[12a^2 + 6k\left(L-\ell\right)^2 + 20k\ell^2\right] - 5k = 0, \end{aligned} \tag{39}$$

$$1224.048\alpha^3 - 944.51\alpha^2 + 17.185\alpha - 0.065 = 0, \tag{40}$$

$$\alpha_{kr1} = -0.753,\ \alpha_{kr2} = 0.0032,\ \alpha_{kr3} = -0.022. \tag{41}$$

At $v_4 = v_1$:

$$\begin{aligned} &16\alpha^3\ell^2 a^2\left(L-\ell\right)^2 - \alpha^2\left[8a^2\left(L-\ell\right)^2 + 48a^2\ell^2 + 12k\ell^2\left(L-\ell\right)^2\right] + \\ &+\alpha\left[12a^2 + 6k\left(L-\ell\right)^2 + 20k\ell^2\right] - 3k = 0, \end{aligned} \tag{42}$$

$$1224.048\alpha^3 - 944.51\alpha^2 + 17.185\alpha - 0.039 = 0, \tag{43}$$

$$\alpha_{kr1} = -0.753,\ \alpha_{kr1} = 0.002,\ \alpha_{kr1} = -0.021. \tag{44}$$

Loss of stability in the horizontal direction at $v_4 = -v_1$ and $k = 0.0013$:

$$1224.05\alpha^3 - 933.827\alpha^2 + 12.538\alpha - 0.007 = 0, \tag{45}$$

$$\alpha_{kr1} = -0.749,\ \alpha_{kr2} = 5.0 \cdot 10^{-4},\ \alpha_{kr3} = -0.014. \tag{46}$$

At $v_4 = v_1$:

$$1224.05\alpha^3 - 933.827\alpha^2 + 12.538\alpha - 0.004 = 0, \tag{47}$$

$$\alpha_{kr1} = -0.749,\ \alpha_{kr2} = 3.0 \cdot 10^{-4},\ \alpha_{kr3} = -0.014. \tag{48}$$

According to the results of approximate methods for determining the critical compressive force, the stability loss of a freight car as a rod system will occur faster in the horizontal direction. With $v_4 = -v_1$, the value of the longitudinal compressive force will be $N_{kr1} = 105.27$ kN, and with $v_4 = v_1$ – $N_{kr1} = 175.45$kN.

Despite the fact that the values of the longitudinal compressive force according to the method of the articulated elastic chain differ significantly from the value obtained earlier, they make it possible to put forward an assumption about the closeness of the values $N_{kri}$for the I and II forms of instability.

It should be noted that the scheme (Fig. 14) requires correction to determine the loss of stability in the vertical direction. The car body rests on the bogies, and when the vertical component of the longitudinal force reaches a certain value, the unloading of the running gear is possible. In this case, the proposed design scheme of the car body as a beam on elasto-yielding supports is a rough approximation.

5.3 Deformation (displacement) method

When considering the stability of a freight car as a rod system (Fig. 15), we solve the problem of instability of I kind (Eulerian instability) with all the accepted assumptions. Since under the action of compressive longitudinal forces a new, bent state is a state of equilibrium, the calculation can be carried out by the force method or the displacement method (Klein et al., 1972; Rabinovich, 1960; Volmir, 1967; Darkov & Shaposhnikov, 1986; Prokofiev & Smirnov, 1948).

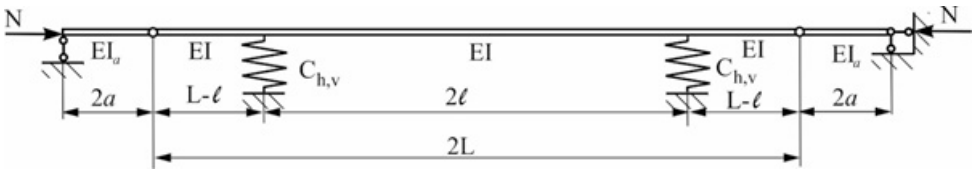

Figure 15: Scheme of a freight car when calculating according to the displacement method

The usual strength calculation of the rod system is carried out according to a non-deformable scheme, while it is assumed that the longitudinal loads in the rods do not affect the value of the bending moments. In fact, due to the bending, these loads cause additional efforts and displacements, which can reach a significant value with large axial loads. To solve the problems of the I and II kind, it is necessary to determine the efforts and displacements in the compressed-bent rods. The most complete table of reactions of compressed-bent rods from single displacements and loads was obtained in the work Klein et al. (1972). All further designations are given in accordance with this work. Therefore, in this section v_i is the critical parameter or length reduction coefficient depending on the instability form. All missing values of reactions from unit displacements and loads were obtained from the solution of the differential bending equation of a compressed-bent rod.

The basic system of the displacement method is obtained from the given one by introducing special additional attachments to all rigid nodes, excluding the supporting ones, and linear connections in the directions identified as a result of the analysis of the dimensional instability of the hinge-rod system. Additional attachments prevent only the rotation of rigid structural nodes and do not prevent their linear displacement. Thus, the rod system in the displacement method has the degree of static indeterminacy equal to 6. Let us take the following designations: $\ell_1 = \ell_5 = 2a$, $\ell_2 = \ell_4 = L - \ell$, $\ell_3 = 2\ell$.

In stability calculations, the use of symmetry is possible only in cases where the frame is not only symmetrical, but also symmetrically loaded. The critical parameters found from the equality to zero of the determinants, composed of the coefficients of the symmetric and skew-symmetric groups of unknowns, constitute the totality of all critical parameters. When searching for the smallest critical forces, this gives a significant reduction in calculations. Taking into account the symmetry of the rod system, the basic system is shown in Fig. 16.

Since the principle of independence of the action of forces is not applicable for transverse-longitudinal bending, the main diagrams are constructed taking into account the influence of the longitudinal force (Fig. 17). Skew-symmetric deformations (II form of instability):

In a bent equilibrium state $z_i \neq 0$, the system of linear homogeneous equations is a non-zero solution only when the determinant, composed of coefficients for unknowns, is equal to zero:

$$D = \frac{6EI}{\ell_2^2} \times \begin{bmatrix} \frac{\eta_1(v_2)}{\ell_2} - \frac{v_1^2 \ell_2^2 k}{3\ell_1^3} & \varphi_1(v_2) & -\frac{\eta_1(v_2)}{\ell_2} \\ \varphi_1(v_2) & \ell_2\varphi_1(v_2) + \frac{2\ell_2^2}{\ell_3}\varphi_4(v_3) & \varphi_1(v_2) - \frac{4\ell_2^2}{\ell_3^2}\varphi_4(v_3) \\ -\frac{\eta_1(v_2)}{\ell_2} & \varphi_1(v_2) - \frac{4\ell_2^2}{\ell_3^2}\varphi_4(v_3) & \frac{\ell_2^2}{3EI}C_{h,v} + \frac{\eta_1(v_2)}{\ell_2} + \frac{8\ell_2^2\eta_2(v_3)}{\ell_3^3} \end{bmatrix} = 0. \quad (49)$$

Hereinafter, the following notations for the functions of the displacement method for compressed-

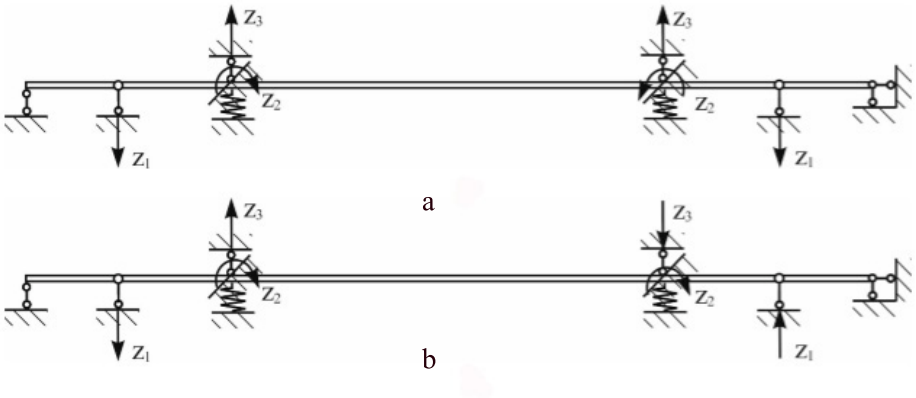

Figure 16: The basic system of the displacement method: a- symmetrical form of instability; b- skew-symmetric form of instability

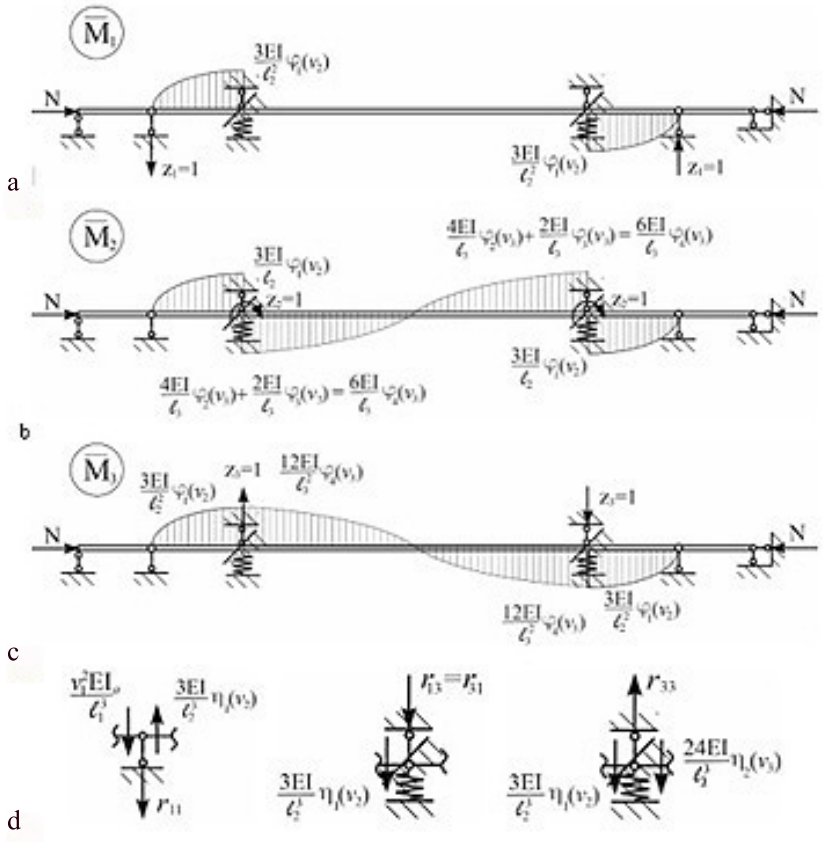

Figure 17: The main diagrams of reaction torque from single displacements in the direction of the chosen unknowns z_i and from the influence of external load: a- diagram $\overline{M_1}$; b- diagram $\overline{M_2}$; c- diagram $\overline{M_3}$; d- a static method for determining the coefficients for unknown

bent rods is adopted:

$$v = \ell \cdot \sqrt{\frac{N}{EI}},\ v_1 = \frac{\ell_1}{\ell_3\sqrt{k}}v_3,\ v_2 = \frac{\ell_2}{\ell_3}v_3, \tag{50}$$

$$\varphi_1(v) = \frac{v^2 tgv}{3(tgv - v)}, \tag{51}$$

$$\varphi_2(v) = \frac{v(tgv - v)}{8tgv\left(tg\,{}^{v}\!/_{2} - {}^{v}\!/_{2}\right)}, \tag{52}$$

$$\varphi_3(v) = \frac{v(v - sinv)}{4sinv\,(tg\,v/2 - v/2)}, \tag{53}$$

$$\varphi_4(v) = \varphi_1(v/2) = \frac{(v/2)^2\, tg\,v/2}{3\,(tg\,v/2 - v/2)}, \tag{54}$$

$$\eta_1(v) = \frac{v^3}{3\,(tgv - v)}, \tag{55}$$

$$\eta_2(v) = \frac{(v/2)^3}{3\,(tg\,v/2 - v/2)}. \tag{56}$$

Having compiled the determinant and equating it to zero, we obtain the stability equation, from which the critical load parameter is determined. Since when the determinant is expanded, a complex transcendental equation is obtained, it is advisable to carry out the calculation separately for the symmetric (I) and skew-symmetric (II) form of instability. The main diagrams for the longitudinal-transverse bending, taking into account the longitudinal force and the symmetrical form of instability, are shown in Fig. 18.

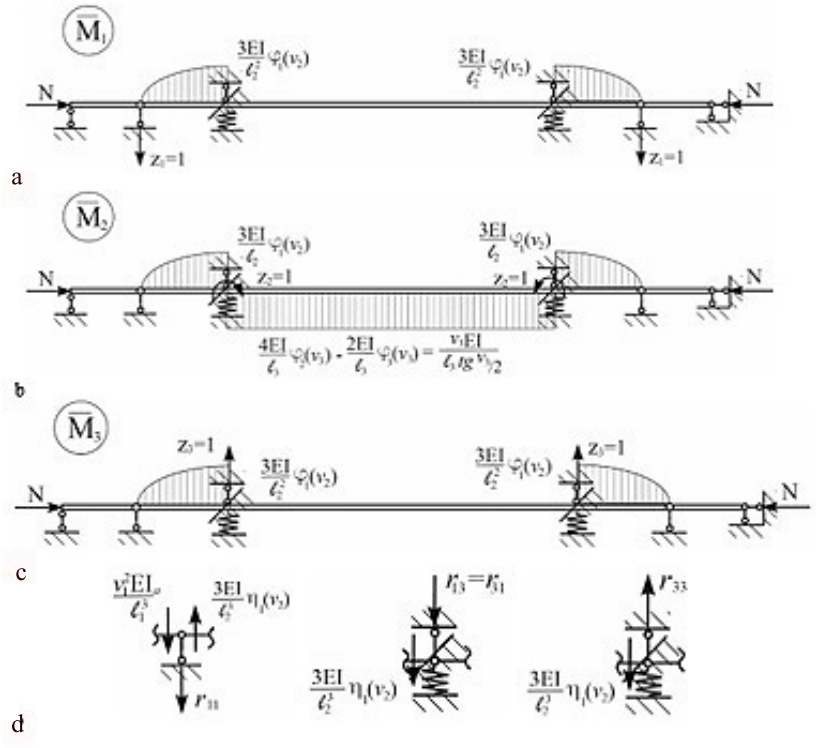

Figure 18: Main diagrams of bending moments from single displacements in the direction of the chosen unknowns z_i and from the influence of external load: a- diagram $\overline{M_1}$; b- diagram $\overline{M_2}$; c- diagram $\overline{M_3}$; d- a static method for determining the coefficients for unknown

The critical load parameter for symmetrical deformation (I form of instability) is determined during expanding the determinant given below:

$$D = \frac{6EI}{\ell_2^2} \times \begin{bmatrix} \frac{\eta_1(v_2)}{\ell_2} - \frac{v_1^2\ell_2^2 k}{3\ell_1^3} & \varphi_1(v_2) & -\frac{\eta_1(v_2)}{\ell_2} \\ \varphi_1(v_2) & \ell_2\varphi_1(v_2) + \frac{v_3\ell_2^2}{3\ell_3 \cdot tg\frac{v_3}{2}} & \varphi_1(v_2) \\ -\frac{\eta_1(v_2)}{\ell_2} & \varphi_1(v_2) & \frac{\ell_2^2}{3EI}C_{h,v} + \frac{\eta_1(v_2)}{\ell_2} \end{bmatrix} = 0. \tag{57}$$

The values of the critical compressive force are determined from the expression:

$$N_{kr} = \frac{v_3^2 EI}{\ell_3^2}. \tag{58}$$

5.4 Determination of the stability loss of a freight car, taking into account its mass

The existing methodology for determining the critical longitudinal forces does not take into account the loading of the car (empty or loaded). At the same time, it has been repeatedly noted that it is the increase in the weight and the length of trains that leads to increased friction of the wheel flanges of cars on the side surface of the rails, track displacement and its removal, an increase in the lateral wear of the rails, flange reduction of wheel sets of cars and even locomotives. Let us consider the body of a four-axle gondola car as an elastic massless beam carrying a uniformly distributed load (Fig. 19).

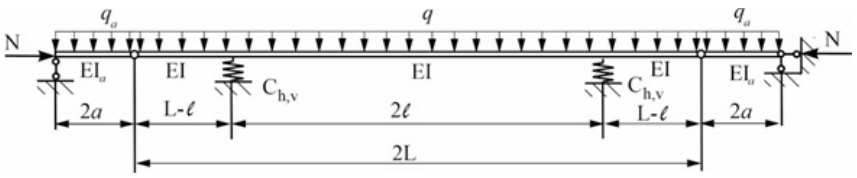

Figure 19: Scheme of a freight car, taking into account its weight and loading mode

Here q_a – own weight of two coupler assemblies, respectively related to two lengths of coupler bodies; q – empty weight of the car body together with the suspended equipment and two bolsters in an empty state, referred to its length. When taking into account the loading, the cargo weight is added to the body weight and is considered to be evenly distributed along the entire length.

Let us consider the instability due to the bending vibrations of the gondola car body as an elastic beam lying on two rigid (spring sets are not compressed and the bolster is taken as a solid body) supports. Such a calculation scheme corresponds to the movement of rolling stock at a speed of less than 60 km/h. The main system of the displacement method, taking into account the symmetry of the rod system, is shown during the car movement at a speed above 60 km/h in Fig. 20, and for the speeds less than 60 km/h in Fig. 20b.

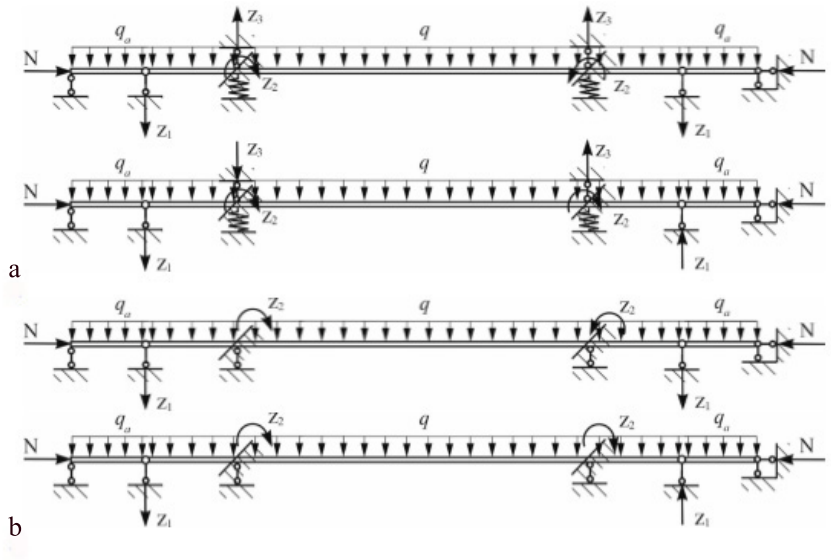

Figure 20: Main system of the displacement method, taking into account the symmetry of the rod system during the car movement: a- above 60 km/h; b- less than 60 km/h.

To determine the coefficients for unknowns in the canonical equations, we build diagrams of reactive bending moments from single displacements in the direction of the chosen unknowns and from the influence of an external load. The main diagrams, taking into account the longitudinal force and the mode of loading the car for skew-symmetric instability forms, are shown in Fig. 21.

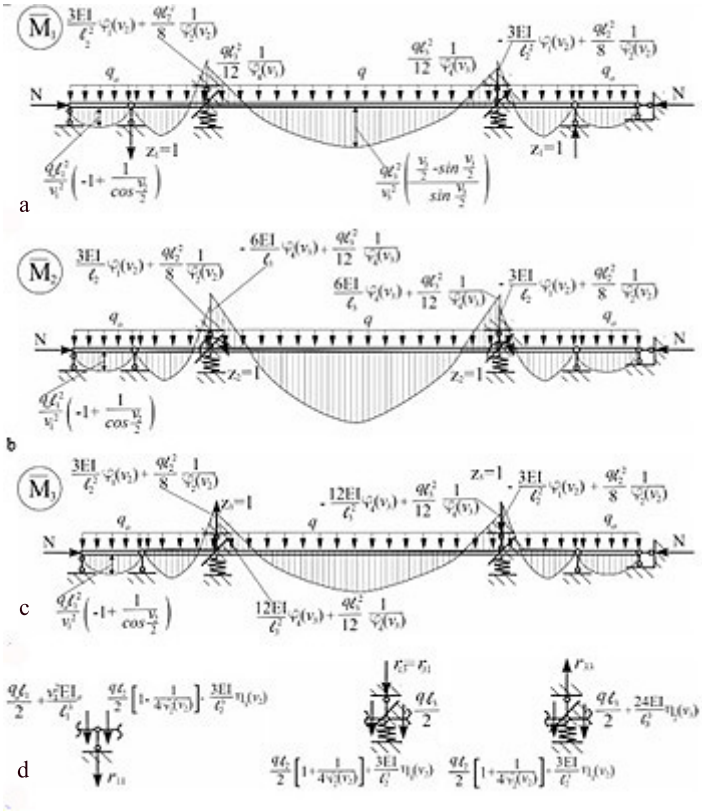

Figure 21: Main diagrams of reactive bending moments from single displacements in the direction of the chosen unknowns $z_i$and from the influence of external load: a- diagram $\overline{M_1}$; b- diagram $\overline{M_2}$; c- diagram $\overline{M_3}$; d- a static method for determining the coefficients for unknowns

When calculating the coefficients for unknowns in canonical equations, we use the reciprocity condition:

$$r_{11} = -\frac{q_a \ell_1}{2} - \frac{v_1^2 EI_0}{\ell_1^3} - \frac{q\ell_2}{2} \cdot \left[1 - \frac{1}{4\varphi_2(v_2)}\right] + \frac{3EI}{\ell_2^3}\eta_1(v_2), \tag{59}$$

$$r_{11}^* = \frac{q_a \ell_1}{2} - \frac{v_1^2 EI_0}{\ell_1^3} + \frac{q\ell_2}{2} \cdot \left[1 - \frac{1}{4\varphi_2(v_2)}\right] + \frac{3EI}{\ell_2^3}\eta_1(v_2), \tag{60}$$

$$r_{12} = \frac{3EI}{\ell_2^2}\varphi_1(v_2) + \frac{q\ell_2^2}{8} \cdot \frac{1}{\varphi_2(v_2)} - \frac{q\ell_3^2}{12} \cdot \frac{1}{\varphi_4(v_3)}, \tag{61}$$

$$r_{12}^* = \frac{3EI}{\ell_2^2}\varphi_1(v_2) - \frac{q\ell_2^2}{8} \cdot \frac{1}{\varphi_2(v_2)} + \frac{q\ell_3^2}{12} \cdot \frac{1}{\varphi_4(v_3)}, \tag{62}$$

$$r_{13} = -\frac{q\ell_3}{2} - \frac{q\ell_2}{2} \cdot \left[1 + \frac{1}{4\varphi_2(v_2)}\right] - \frac{3EI}{\ell_2^3}\eta_1(v_2), \tag{63}$$

$$r_{13}^* = \frac{q\ell_3}{2} + \frac{q\ell_2}{2} \cdot \left[1 + \frac{1}{4\varphi_2(v_2)}\right] - \frac{3EI}{\ell_2^3}\eta_1(v_2), \tag{64}$$

$$r_{22} = \frac{6EI}{\ell_3}\varphi_4(v_3) - \frac{q\ell_3^2}{12} \cdot \frac{1}{\varphi_4(v_3)} + \frac{q\ell_2^2}{8} \cdot \frac{1}{\varphi_2(v_2)} + \frac{3EI}{\ell_2}\varphi_1(v_2), \tag{65}$$

$$r_{22}^* = \frac{6EI}{\ell_3}\varphi_4(v_3) + \frac{q\ell_3^2}{12} \cdot \frac{1}{\varphi_4(v_3)} - \frac{q\ell_2^2}{8} \cdot \frac{1}{\varphi_2(v_2)} + \frac{3EI}{\ell_2}\varphi_1(v_2), \tag{66}$$

$$r_{23} = -\frac{12EI}{\ell_3^2}\varphi_4(v_3) - \frac{q\ell_3^2}{12} \cdot \frac{1}{\varphi_4(v_3)} + \frac{3EI}{\ell_2^2}\varphi_1(v_2) + \frac{q\ell_2^2}{8} \cdot \frac{1}{\varphi_2(v_2)}, \tag{67}$$

$$r_{23}^{*} = -\frac{12EI}{\ell_3^2}\varphi_4(v_3) + \frac{q\ell_3^2}{12}\cdot\frac{1}{\varphi_4(v_3)} + \frac{3EI}{\ell_2^2}\varphi_1(v_2) - \frac{q\ell_2^2}{8}\cdot\frac{1}{\varphi_2(v_2)}, \tag{68}$$

$$r_{33} = C_{h,v} + \frac{q\ell_2}{2}\cdot\left[1 + \frac{1}{4\varphi_2(v_2)}\right] + \frac{3EI}{\ell_2^3}\eta_1(v_2) + \frac{q\ell_3}{2} + \frac{24EI}{\ell_3^3}\eta_2(v_3), \tag{69}$$

$$r_{33}^{*} = C_{h,v} - \frac{q\ell_2}{2}\cdot\left[1 + \frac{1}{4\varphi_2(v_2)}\right] + \frac{3EI}{\ell_2^3}\eta_1(v_2) - \frac{q\ell_3}{2} + \frac{24EI}{\ell_3^3}\eta_2(v_3). \tag{70}$$

As noted earlier, when searching for the smallest critical forces of a symmetric and symmetrically loaded system, it suffices to find two smaller critical parameters for a directly symmetric and skew-symmetric grouping of unknowns. The critical parameter v_3 for the skew-symmetric instability form (II form) with a directly symmetric grouping of unknowns, taking into account the loading of the car (empty or loaded), is determined by expanding the determinant, composed of expressions for the coefficients at unknowns of the dependencies:

$$r_{11} = 2\cdot\left[-\frac{v_1^2 EI_0}{\ell_1^3} + \frac{3EI}{\ell_2^3}\eta_1(v_2)\right], \tag{71}$$

$$r_{12} = r_{21} = 2\cdot\frac{3EI}{\ell_2^2}\varphi_1(v_2), \tag{72}$$

$$r_{13} = r_{31} = -2\cdot\frac{3EI}{\ell_2^3}\eta_1(v_2), \tag{73}$$

$$r_{22} = 2\cdot\left[\frac{6EI}{\ell_3}\varphi_4(v_3) + \frac{3EI}{\ell_2}\varphi_1(v_2)\right], \tag{74}$$

$$r_{23} = r_{32} = 2\cdot\left[-\frac{12EI}{\ell_3^2}\varphi_4(v_3) + \frac{3EI}{\ell_2^2}\varphi_1(v_2)\right], \tag{75}$$

$$r_{33} = 2\cdot\left[C_{h,v} + \frac{3EI}{\ell_2^3}\eta_1(v_2) + \frac{24\eta_2(v_3)}{\ell_3^3}\right]. \tag{76}$$

The obtained expressions for the coefficients of unknowns are completely identical to the determinant (49), which allows us to put forward the assumption that the weight of both the car itself and the load in it does not affect the value of the longitudinal compressive force for skew-symmetric instability forms. The second stability equation for a skew-symmetric grouping of unknowns is obtained from the difference between the coefficients (59)-(70).

The calculation scheme of a gondola car as an elastic beam lying on two rigid supports, corresponding to the movement of rolling stock at the speeds up to 60 km/h, makes it possible to obtain a critical parameter $v_3$when expanding the determinant:

$$D = 2EI\cdot\begin{vmatrix} \frac{3}{\ell_2^3}\eta_1(v_2) - \frac{v_1^2\cdot k}{\ell_1^3} & \frac{3}{\ell_2^2}\varphi_1(v_2) \\ \frac{3}{\ell_2^2}\varphi_1(v_2) & \frac{6EI}{\ell_3}\varphi_4(v_3) + \frac{3}{\ell_2}\varphi_1(v_2) \end{vmatrix} = 0. \tag{77}$$

As a result, we obtain the transcendental equation:

$$\left(\frac{3}{\ell_2^3}\eta_1(v_2) - \frac{v_1^2\cdot k}{\ell_1^3}\right)\cdot\left(\frac{6EI}{\ell_3}\varphi_4(v_3) + \frac{3}{\ell_2}\varphi_1(v_2)\right) - \left(\frac{3}{\ell_2^2}\varphi_1(v_2)\right)^2 = 0. \tag{78}$$

The main diagrams, taking into account the longitudinal force and the mode of car loading for the symmetrical form of instability, are given in Fig. 22.

Using the reciprocity condition when calculating the coefficients of the unknowns in the canonical equations, we obtain:

$$r_{11} = 2\cdot\left[-\frac{q_a\ell_1}{2} - \frac{v_1^2 EI_0}{\ell_1^3} - \frac{q\ell_2}{2}\cdot\left[1 - \frac{1}{4\varphi_2(v_2)}\right] + \frac{3EI}{\ell_2^3}\eta_1(v_2)\right], \tag{79}$$

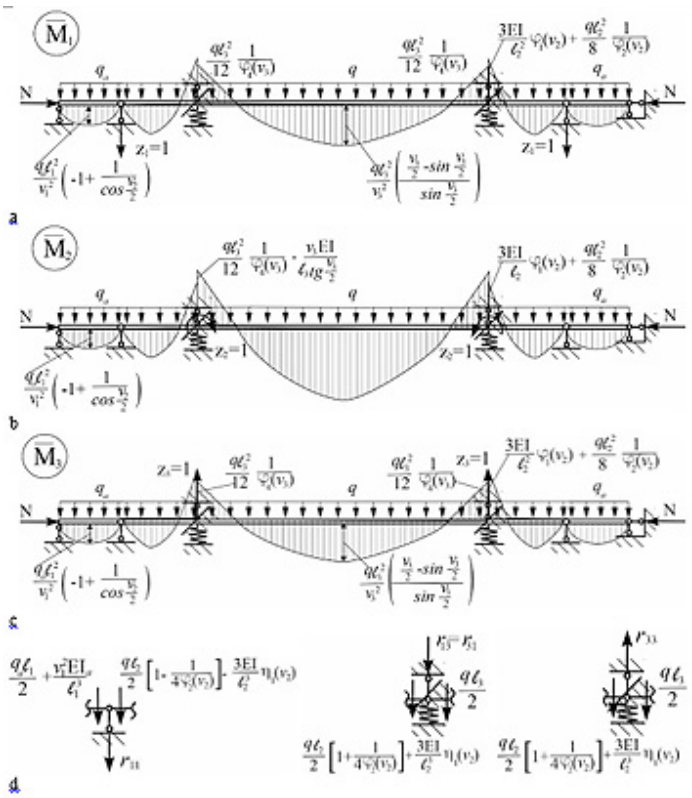

Figure 22: Main diagrams of reactive bending moments from single displacements in the direction of the chosen unknowns z_i and from the influence of external load: a- diagram $\overline{M_1}$; b- diagram $\overline{M_2}$; c- diagram $\overline{M_3}$; d- a static method for determining the coefficients for unknowns

$$r_{21} = r_{12} = 2 \cdot \left[\frac{3EI}{\ell_2^2} \varphi_1 (v_2) + \frac{q\ell_2^2}{8} \cdot \frac{1}{\varphi_2 (v_2)} - \frac{q\ell_3^2}{12} \cdot \frac{1}{\varphi_4 (v_3)} \right], \tag{80}$$

$$r_{13} = r_{31} = 2 \cdot \left[-\frac{q\ell_3}{2} - \frac{q\ell_2}{2} \cdot \left[1 + \frac{1}{4\varphi_2 (v_2)} \right] - \frac{3EI}{\ell_2^3} \eta_1 (v_2) \right], \tag{81}$$

$$r_{22} = 2 \cdot \left[\frac{v_3 EI}{\ell_3 tg^{v_3}/_2} - \frac{q\ell_3^2}{12} \cdot \frac{1}{\varphi_4 (v_3)} + \frac{q\ell_2^2}{8} \cdot \frac{1}{\varphi_2 (v_2)} + \frac{3EI}{\ell_2} \varphi_1 (v_2) \right], \tag{82}$$

$$r_{23} = r_{32} = 2 \cdot \left[\frac{3EI}{\ell_2^2} \varphi_1 (v_2) + \frac{q\ell_2^2}{8} \cdot \frac{1}{\varphi_2 (v_2)} - \frac{q\ell_3^2}{12} \cdot \frac{1}{\varphi_4 (v_3)} \right], \tag{83}$$

$$r_{33} = 2 \cdot \left[C_{h,v} + \frac{q\ell_2}{2} \cdot \left[1 + \frac{1}{4\varphi_2 (v_2)} \right] + \frac{3EI}{\ell_2^3} \eta_1 (v_2) + \frac{q\ell_3}{2} \right]. \tag{84}$$

The critical parameterv_3 for the symmetric form of instability (I form) is determined by expanding the determinant, composed of expressions for the coefficients of unknowns according to the dependencies (79)-(84). Similarly to the previous calculation of a gondola car as an elastic beam lying on two rigid supports, we obtain the critical parameter v_3 when taking out the multiplier $2EI$ and expanding the determinant:

$$\begin{vmatrix} \frac{3\eta_1(v_2)}{\ell_2^3} - \frac{q_a \ell_1}{2EI} - \frac{v_3^2}{\ell_3^2 \ell_1} - \frac{q\ell_2}{2EI} \left[1 - \frac{1}{4\varphi_2(v_2)} \right] & \frac{3\varphi_1(v_2)}{\ell_2^2} + \frac{q\ell_2^2}{8EI\varphi_2(v_2)} - \frac{q\ell_3^2}{12EI\varphi_4(v_3)} \\ \frac{3\varphi_1(v_2)}{\ell_2^2} + \frac{q\ell_2^2}{8EI\varphi_2(v_2)} - \frac{q\ell_3^2}{12EI\varphi_4(v_3)} & \frac{v_3}{\ell_3 tg^{v_3}/_2} - \frac{q\ell_3^2}{12EI\varphi_4(v_3)} + \frac{q\ell_2^2}{8EI\varphi_2(v_2)} + \frac{3\varphi_1(v_2)}{\ell_2} \end{vmatrix} = 0. \tag{85}$$

As a result, we obtain the transcendental equation:

$$\left(\frac{3\eta_1(v_2)}{\ell_2^3}-\frac{q_a\ell_1}{2EI}-\frac{v_3^2}{\ell_3^2\ell_1}-\frac{q\ell_2}{2EI}\left[1-\frac{1}{4\varphi_2(v_2)}\right]\right)\cdot\left(\frac{v_3}{\ell_3 tg\,v_3/2}-\frac{q\ell_3^2}{12EI\varphi_4(v_3)}+\frac{q\ell_2^2}{8EI\varphi_2(v_2)}+\frac{3\varphi_1(v_2)}{\ell_2}\right)-$$
$$-\left(\frac{3\varphi_1(v_2)}{\ell_2^2}+\frac{q\ell_2^2}{8EI\varphi_2(v_2)}-\frac{q\ell_3^2}{12EI\varphi_4(v_3)}\right)^2=0. \tag{86}$$

5.5 Determination of the stability loss of a freight car, taking into account the skew in relation to neighboring carriages in the coupling

As already indicated, the cars almost always have some skew in plan relative to each other due to the hunting of carriages, gaps in the track, spring units, axle boxes and center plate arrangements, and for other reasons (Lysyuk, 2002; Sokol, 2002; Lazaryan et al., 1966; Vershinskiy, 1970; Shvets et al., 2016, 2020, 2015). Let us consider a car with central automatic couplers of shock-traction action as a multi-link articulated-rod chain, taking into account possible displacement in relation to the neighboring carriages in the coupling.

Since it was established by the previous studies that accounting of the car loading (empty or loaded) does not affect the critical parameter v_3 for the skew-symmetric instability form (II form), then during the expansion of the determinant (49) for the scheme of cars arrangement in the train in Fig. 3a it is necessary to use the expression for the coefficient r_{11}:

$$r_{11}^a=2\cdot\left[-\frac{2v_1^2EI_0}{\ell_1^3}+\frac{3EI}{\ell_2^3}\eta_1(v_2)\right]=\frac{6EI}{\ell_2^2}\times\left[\frac{\eta_1(v_2)}{\ell_2}-\frac{2v_1^2\ell_2^2k}{3\ell_1^3}\right]. \tag{87}$$

For the scheme in Fig. 3c:

$$r_{11}^c=2\cdot\frac{3EI}{\ell_2^3}\eta_1(v_2)=\frac{6EI}{\ell_2^2}\times\frac{\eta_1(v_2)}{\ell_2}. \tag{88}$$

For the scheme of the car arrangement in the case of a symmetrical instability form (Fig. 3b), when transferring the longitudinal force, the coefficient r_{11} is determined by the following dependence:

$$r_{11}^b=2\cdot\left[-\frac{q_a\ell_1}{2}-\frac{2v_1^2EI_0}{\ell_1^3}-\frac{q\ell_2}{2}\cdot\left[1-\frac{1}{4\varphi_2(v_2)}\right]+\frac{3EI}{\ell_2^3}\eta_1(v_2)\right]. \tag{89}$$

The critical parameter v_3 for the symmetric form of instability (I form) is determined by expanding the determinant, composed of expressions for the coefficients of unknowns according to the dependencies (89) and (80)-(84).

The given methodology for determining the instability form of a car in a train under the action of the compressive longitudinal forces is rather cumbersome. The numerical solution of the obtained transcendental equations will make it possible to compare with the results of approximate calculation methods, as well as to conclude about the possibility of their application. In addition, it is enough to solve the transcendental equations only once for a certain model or a group of models close in technical (geometric, mass, inertial) characteristics.

6 Conclusion

The process of interaction between the rolling stock and the track superstructure is determined by many factors: the slopes and curved track sections, the weight, length and speed of trains, the power of a locomotive or a group of locomotives, that is, the maximum braking force. The concentration of a large braking force (up to 80% of the maximum traction force) on a short track section (the locomotive length) in the head of the train and the closing up of unbraked

rear cars contribute to the skewed location of the cars of the first train third in a track. The latter leads to an increase in the flange friction of the wheel sets of cars on the side surface of the rails, track displacement and its removal, an increase in lateral wear of the rails, flange reduction of wheel sets of cars and even locomotives. An increase in the weight and length of trains sharply worsens the situation under consideration. The study of the influence of the longitudinal forces value of a quasi-static nature on the form of instability of cars in a train and the stability of wheel sets of freight cars in the process of operational work is one of the priority tasks for improving the technology of driving trains. Based on the behavioral analysis, the following conclusions can be made:

– the loss of stability of freight cars in the train should be divided into two stages: the loss of the body stability on the spring suspension and the loss of the wheel set stability, which leads directly to the derailment;

– currently used calculation scheme of the car body as a beam on elasto-yielding supports in the vertical plane is a rough approximation;

– in the process of theoretical studies, dependencies were obtained to determine the critical parameter, which depends on the form of instability, taking into account the stiffness and weight of the elements of the hinge-rod system under study;

– the use of the above methodology for determining the critical parameter for the I and II forms of instability under the action of quasi-static longitudinal forces will allow us to justify the cause of derailment, as well as to develop and put into practice the technical measures to prevent the lift of the carriages, widening and shear of the track;

– the given methodology for determining the stability coefficient against car lift by longitudinal forces has a high convergence with the results of an experiment carried out under similar conditions;

– in order to carry out continuous analysis in train conditions of the value of the resulting longitudinal compressive forces and to prevent large compressive forces, it is necessary to equip locomotives with a system for monitoring and recording longitudinal forces arising on the automatic coupler of the locomotive;

– the longitudinal force in front and behind the car is usually not the same and has some increment. Taking into account the difference in the values of the longitudinal force will allow, to some extent, to answer the question which of the design schemes of the longitudinal compressive forces should be applied in each specific case under consideration when determining the derailment stability coefficient.

The fact that the instability of the cars occurs both according to I and II form indicates a significant intensity influence of the increase in the value of the longitudinal force in a short period of time. It is possible to assume that a slow increase leads to instability of II form, a fast one – to the instability of I form.

The use of the above methodology in compiling the process flow diagrams for driving the trains will make it possible to recommend rational train driving not only at the lowest energy costs, but to implement technical measures to improve the stability of freight rolling stock, which in turn will allow removing some existing restrictions on permissible speeds and increasing the train speed.

When conducting research on the dynamic interaction of the rolling stock and the track, the forces acting on a particular car in the train are of particular interest. Therefore, when conducting further research, it is advisable to confine oneself to considering the movement of only a group of cars that forms its certain neighborhood. Since it is impossible to set the boundary conditions exactly at the boundaries of the group, it is necessary to investigate how many cars should form the neighborhood of the car under study, so that inaccurate boundary conditions do not significantly affect the calculation results.

References

Blokhin, Ye.P., Vershinskiy, S.V. (1985). *Determination of additional lateral forces of the impact of cars on the track, caused by longitudinal forces in heavy and long trains.* Research report No. 299 from the archive of BRL DSRS of the Dnipro National University of Railway Transport.

Darkov, A.V., Shaposhnikov, N.N. (1986). *Structural Mechanics.* Moscow, High school.

In the Odessa region, a freight train derailed [online] [accessed 2021-09-15]. Available from: https://www.rbc.ua/rus/news/odesskoy-oblasti-soshel-relsov-gruzovoy-poezd-1530633610.html

Kampczyk, A., Dybel, K. (2021). Integrating surveying railway special grid pins with terrestrial laser scanning targets for monitoring rail transport infrastructure. *Measurement*, 170, 108729.

Klein, G.K., Rekach, V.G. & Rosenblat, G.I. (1972). *Guide to practical exercises in the course of structural mechanics. Fundamentals of the theory of stability, dynamics of structures and calculation of spatial systems.* Moscow, Higher School Publishing House.

Kovalchuk, V., Sysyn, M., Gerber, U., Nabochenko, O., Zarour, J., & Dehne, S. (2019). Experimental investigation of the influence of train velocity and travel direction on the dynamic behavior of stiff common crossings. *Facta Universitatis. Series: Mechanical Engineering, 17*(3), 345-356.

Kurhan, M., Kurhan, D. (2019). Providing the railway transit traffic Ukraine-European Union. *Pollack Periodica, 14*(2), 27-38.

Kurhan, M.B., Kurhan, D.M., Husak, M.A., & Hmelevska, N. (2022). Increasing the Efficiency of the Railway Operation in the Specialization of Directions for Freight and Passenger Transportation. *Acta Polytechnica Hungarica*, *19*(3), 231–244.

Kurhan, M.B., Kurhan, D.M., & Cerniauskaite, L. (2019). Rationale of priority areas of rail operation in north-eastern Europe. *Proceedings of the 23rd International Scientific Conference on Transport Means*, Lithuania, 1439–1444.

Lazaryan, V.A. (1952). On the selection of design scheme in the study of transient regimes of train movement. *Railway engineering*, 6, 17–19.

Lazaryan, V.A. (1953). Investigations of transient modes of train movement during continuous braking and during transitions through fractures of the longitudinal profile of the track. *Works of DIIT*, 23, 5–23.

Lazaryan, V.A. (1956). Investigation of the forces arising during transient modes of motion in rods with various elastic imperfections. *Works of DIIT*, 25, 5–50.

Lazaryan, V.A., Blokhin, Ye.P., & Stambler, Ye.L. (1966). *About motion of lightweight cars in the heavy trains.* Dnipropetrovsk: DIIT.

Lazaryan, V.A. (1985). *Vehicle Dynamics: Selected Works.* Kyiv, Naukova Dumka.

Lysyuk, V.S. (2002). *The causes and mechanisms of the vanishing wheel from the rail. The problem of wear of wheels and rails.* Moscow: Publisher Transport, .

Prokofiev, I.P., Smirnov, A.F. (1948). *Theory of Structures. Part 3.* Moscow, State Railway Transport Publishing House.

Qi, Z., Huang, Z., & Kong, X. (2012). Simulation of longitudinal dynamics of long freight trains in positioning operations. *Vehicle system dynamics, 50*(9), 1409-1433.

Rabinovich, I.M. (1960). *Fundamentals of structural mechanics of rod systems.* Moscow, Stroyizdat.

Shaposhnik, V.Yu., Shikunov, O.A. (2021). The problem of breaks automatic coupling. *Coll. Science. Ave. University of Infrastructure and Technology. Series: Transp. systems and technologies*, 37, 21–30. DOI:10.32703/2617-9040-2021-37-3

Shaukat, A.R., Lan, P., Wang, J., Wang, T. (2021). In-plane nonlinear postbuckling analysis of circular arches using absolute nodal coordinate formulation with arc-length method. *Proc IMechE Part K: J Multi-body Dynamics*, *235*(3), 297–311. DOI:10.1177/1464419320971412

Shvets, A.O., Zhelieznov, K.I., Akulov, A.S., Zabolotnyi, O.M., & Chabaniuk, E.V. (2015). Some aspects of the definition of empty cars stability from squeezing their longitudinal forces in the freight train. *Science and Transport Progress, 4*(58), 175-189.

Shvets, A.A., Zheleznov, K.I., Akulov, A.S. et al. (2016). Determination the permissible forces in assessing the lift resistant factor of freight cars in trains. *Science and Transport Progress*, *1*(61), 189–192. DOI:10.15802/stp2016/61045

Shvets, A.O. (2020). Stability of freight wagons under the action of compressing longitudinal forces. *Science and Transport Progress*, 1(85), 119–137. DOI:10.15802/stp2020/199485

Shvets, A.O. (2021a). Analysis of the dynamics of freight cars with lateral displacement of the front bogie. *Advanced Mathematical Models & Applications*, *6*(1), 45–58.

Shvets, A.O. (2021b). Dynamic interaction of a freight car body and a three-piece bogie during axle load increase. *Vehicle System Dynamics* published online: 2021-07-07; doi.org/10.1080/00423114.2021.1942930.

Shvets, A.O., Shatunov, O.V., Dovhaniuk, S.S., Muradian, L.A., Pularyia, A.L., & Kalashnik, V.V. (2020, November). Coefficient of stability against lift by longitudinal forces of freight cars in trains. In *IOP Conference Series: Materials Science and Engineering* (Vol. 985, No. 1, p. 012025).

Sokol, E.N. (2002). *Derailment and collision of rolling stock.* Kiev: Transport of Ukraine.

Travel disruption as freight train derails near Coleshill [online] [accessed 2021-09-15]. Available from: https://www.bbc.com/news/uk-england-45508412

Ursulyak, L., Shvets, A. (2017). Improvement of mathematical models for estimation of train dynamics. *Science and Transport Progress*, *6*(72), 70–82. DOI:10.15802/stp2017/118002

Ushkalov, V.F. (1965). *Investigation of flexural vibrations of freight car bodies, Dnepropetrovsk Institute of Transport Engineers.* Dnepropetrovsk, DIIT.

Vershinskiy, S.V. (1970). Dynamics, durability and the stability of cars in heavy and high-speed trains. Sbornik trudov VNIIZhTa, Moscow: Transport Publ.

Vershinskiy, S.V., Danilov, V.I. & Chelnokov, I.I. (1991). *Dynamics of cars.* Moscow, Transport Publ.

Volmir, A.S. (1967). *Stability of Deformable Systems. Second edition, revised and enlarged.* Moscow, Nauka.

Wu, Q., Cole, C., & Spiryagin, M. (2018). Assessing wagon pack sizes in longitudinal train dynamics simulations. *Australian Journal of Mechanical Engineering*, 18(3), 277-287.

Wu, Q., Spiryagin, M., & Cole, C. (2016). Longitudinal train dynamics: an overview. V*ehicle System Dynamics, 54*(12), 1688-1714.

Zhang, H., Zhang, C., Lin, F., Wang, X., & Fu, G. (2021). Research on Simulation Calculation of the Safety of Tight-Lock Coupler Curve Coupling. *Symmetry, 13*(11), 1997. DOI:10.3390/sym13111997

Zhang, S., Shi, W., Wu, Z., et al. (2022). Continuum damage dynamics of a large-scale flexible multibody system comprised of compo site beams. *Proc. IMechE Part K: J Multi-body Dynamics*, *236*(2), 205–223. DOI:10.1177/ 146441932110 63179